Natural Hazards
https://doi.org/10.1007/s11069-019-03645-w

ORIGINAL PAPER

Nonstationary joint probability analysis of extreme marine variables to assess design water levels at the shoreline in a changing climate

Panagiota Galiatsatou[1] · Christos Makris[1] · Panayotis Prinos[1] · Dimitrios Kokkinos[1]

Received: 29 December 2017 / Accepted: 19 June 2019

Abstract
In the present study, a recently developed novel approach (Bender et al. in J Hydrol 514:123–130, 2014) has been further extended to investigate the changes in the joint probabilities of extreme offshore and nearshore marine variables with time and to assess design the total water level (TWL) at the shoreline under the effects of climate change. The nonstationary generalised extreme value (GEV) distribution has been utilised to model the marginal distribution functions of marine variables (wave characteristics and sea levels), within a 40-year moving window. All parameters of the GEV were tested for statistically significant linear and polynomial trends over time, and best-fitted trends have been detected. Different copula functions were fitted at the 40-year moving windows, to model the dependence structure of extreme offshore significant wave heights and peak spectral periods, and of wave-induced sea levels on the shoreline and nearshore sea levels due to storm surges. The most appropriate bivariate models were then selected. Statistically significant polynomial trends were detected in the dependence parameters of the selected copulas, and time-dependent most likely bivariate events were extracted to be used in the estimation of the TWL at the shoreline. The methods of the present work were implemented in three selected Greek coastal areas in the Aegean Sea. The analysis revealed different variations in the most likely estimates of the offshore wave characteristics and nearshore storm surges in the three study areas, as well as in the time-dependent estimates of TWL at the shoreline. The approach combines nonstationarity and bivariate analysis, blends coastal and offshore marine features and finally provides non-trivial alterations in the response of coastal sea level dynamics to climate change signals, compared to former work on the subject. The methodology produces reasonable estimates of design quantities for coastal structures and boundary conditions for the assessment of flood hazard and risk in coastal areas.

Keywords Extremes · Nonstationary · Joint probability · Copula · Total water level · Coastal hazard · Climate change · Wave · Storm surge

✉ Panagiota Galiatsatou
pgaliats@civil.auth.gr

[1] Division of Hydraulics and Environmental Engineering, School of Civil Engineering, Aristotle University Of Thessaloniki, 54124 Thessaloníki, Greece

1 Introduction

Extreme marine events can give rise to serious coastal flooding and have severe impacts on human society, as well as on the environment. The general inception of a changing climate with extreme marine events of higher frequency and intensity and mean sea level (MSL) rise are expected to increase exposure and vulnerability of society, infrastructure and the environment of coastal areas to severe damages. The threat of climate change, combined with high concentration of economic activities and other assets in coastal areas with high significance for national economic performance and development of most countries, creates an urgent need to understand and manage the risks associated with future extreme marine events that can cause extended coastal inundation.

1.1 Literature review

The effect of climate change on the coastal zone is mostly associated with MSL rise, together with significant changes in the trajectories, intensity and frequency of occurrence of severe storm events that can cause extreme positive surges (IPCC 2007, 2012). Although the majority of scientific studies in the Mediterranean have focused on the variability and long-term trends in MSL (Marcos and Tsimplis 2008; Somot et al. 2008; Carillo et al. 2012; Tsimplis et al. 2013; Adloff et al. 2015), changes in extreme storm surges and waves under the effects of climate change started to receive considerable attention quite recently. Gaertner et al. (2007) detected the danger of a tropical cyclone above the Mediterranean accounting for future climate change, using different high-resolution Regional Climate Models (RCMs). Indications of climate change effects on storm wave events in the Mediterranean have been investigated by several researchers; selected ones are listed as follows: Lionello et al. (2008) detected milder marine storms for the period 2071–2100 in the future A2 and B2 emission scenarios, compared to those of the present climate, apart for the summer period in the central Mediterranean under A2 scenario. Martucci et al. (2010) detected a negative trend in the annual- and winter-averaged sea state heights derived from the European Centre for Medium Range Weather Forecasts (ECMWF) WAve Model (WAM) forced by ECMWF's Re-Analysis (ERA-40) datasets in selected areas of the Italian coast, and there is no significant change in sea state durations exceeding certain thresholds. Benetazzo et al. (2012) estimated a generally milder wave climate for the Adriatic Sea during the 2070–2099 future period, even though wave extremes severity might intensify locally. Casas-Prat and Sierra (2011, 2013) projected the extreme wave climate of the northwestern Mediterranean Sea obtaining changes of up to $\pm 20\%$, with mirrored variations in wave periods and heights, due to limited fetches in their study area; thus, there are insignificant changes in wind wave/swell distributions. Galiatsatou and Prinos (2014, 2015), Androulidakis et al. (2015), Galiatsatou et al. (2016) and Makris et al. (2016) studied the impacts of climate change on extremes of marine characteristics (storm surge-induced sea levels and spectral wave characteristics) in selected areas of the east-central Mediterranean, Aegean and Ionian Seas, detecting a considerable increase in the extreme wave climate and extreme storm surges in the North Aegean and the Ionian Seas in the first half of the twenty-first century.

Recent studies on Extreme Value Analysis (EVA) for variables associated with the marine and coastal environment have been published by different researchers. Méndez et al. (2006) presented a time-dependent version of the peaks-over-threshold (POT) model,

allowing it to consider trends, annual cycles and metocean covariates to analyse variability in extreme wave climate, while Méndez et al. (2008) introduced a version of the model accounting for seasonality and conditioning to the duration of the storm event. Van Gelder and Mai (2008) identified the main methods for estimating the distribution functions for wave height and storm surge extremes at the Dutch coast in the North Sea area, implementing extreme value theory (EVT). Sánchez-Arcilla et al. (2008) studied extreme wave events using a conventional extreme value (EV) and a Bayesian approach, indicating how the introduction of a priori knowledge in EVA helps to reduce uncertainty in predictions of extremes. Bulteau et al. (2013) performed spatial EVA of significant wave height along the French coast using different EV techniques. Jonathan et al. (2014a) presented a novel method to estimate return levels of significant wave height for storm peak events in large areas, incorporating spatial and directional effects. Sartini et al. (2017) investigated the spatial variability of extreme significant wave heights in the Mediterranean Sea by means of a point-wise EV distribution including covariates representing the meteorological forcing and identified four modes of variability of the wave climate in the area. EV methods have been also implemented for studying the statistical characteristics of storm surge, mainly in the North Sea area (i.e. van Gelder 1999; Coles and Tawn 2005; Butler et al. 2007; Galiatsatou and Prinos 2008; Sterl et al. 2009; Gaslikova et al. 2013; Ridder et al. 2018). Bardet et al. (2011) presented a regional frequency analysis of extreme storm surges along the French coast, leading to more reliable estimates compared to at-site analysis. Lopeman et al. (2015) applied the Clustered Separated Peaks-over-threshold Simulation (CSPS) method to estimate extreme storm surges of Hurricane Sandy at the coast of lower Manhattan, New York, managing to provide a more reliable estimate for the return period of the hurricane's peak water level.

Although extremes of marine variables, such as wave heights, wave periods and water levels, have been considered by numerous authors, studies on the combined impact of such variables are more limited. Morton and Bowers (1996), De Haan and De Ronde (1998), Ferreira and Guedes Soares (2002), Repko et al. (2004), Yeh et al. (2006) and Callaghan et al. (2008) described the joint probability distribution function of long-term hydraulic conditions. Galiatsatou (2007) compared different pairs of bivariate observations of extreme waves and storm surges with reference to joint exceedance probabilities, in order to find the most severe sea state caused by the two variables. McInnes et al. (2009) presented an approach for evaluating storm tide return levels, applying a joint probability method to analyse tides and storm surge heights under present and future climate conditions. Wahl et al. (2012) jointly analysed storm surge parameters, such as highest turning point and intensity with the significant wave height, by means of Archimedean copulas, resulting in reliable exceedance probability estimates. Corbella and Stretch (2013) investigated dependencies between wave height, wave period, storm duration, water level and storm inter-arrival time and used trivariate copulas to jointly analyse the variables that are significantly associated. Gouldby et al. (2014) introduced a practical approach for simulating extreme nearshore sea conditions utilising modern statistical techniques, including the generation of a large sample of offshore sea conditions using the conditional extremes model of Heffernan and Tawn (2004) and the development of a meta-model of the wave transformation process. Jonathan et al. (2014b) presented a nonstationary joint modelling approach using multidimensional covariates based on the conditional extremes model of Heffernan and Tawn (2004) and applied it to the significant wave height and associated peak spectral period of the extra-tropical storm peak, with storm direction as covariate. Serafin and Ruggiero (2014) and Serafin et al. (2017) introduced a total water level (TWL) full simulation model (TWL-FSM) that considers the seasonal and interannual climatic

variability in extreme marine events, while taking into account conditional dependencies between the different components of TWL in a Monte Carlo framework, in order to investigate the relative contribution of the different marine variables to extreme TWL on US West Coast sandy beaches. Masina et al. (2015) produced the joint probability distribution of extreme water levels and wave heights at Ravenna coast in Italy and used the direct integration method to assess the flooding probability. Hsu et al. (2018) developed an approach based on the joint probability method with optimal sampling using surge response functions to predict extreme surge elevations as a function of hurricane parameters and to assess impacts of the estimated storm surge hazard at three study sites in the northern Gulf of Mexico. Mazas and Hamm (2017) presented an approach for determining extreme joint probabilities of wave heights and sea levels focusing on the sampling of the two variables, proposed to be based on the event generating the variables or resulting from their combined effect.

Copulas were widely used in the analysis of multivariate extremes both in hydrology and in marine studies (i.e. Grimaldi and Serinaldi 2006; Shiau 2006; De Michele et al. 2007; Kao and Govindaraju 2008; AghaKouchak et al. 2010; Salvadori and De Michele 2010; Salvadori et al. 2011; Janga Reddy and Ganguli 2012; Zhong et al. 2013; Li et al. 2014; Rueda et al. 2016; Wahl et al. 2016; Mazas and Hamm 2017). However, the majority of such studies considered stationarity of the marginal parameters and of the dependence structure of the copula. Singh and Zhang (2007), Corbella and Stretch (2013) and Chebana et al. (2013) investigated the use of nonstationary marginal distributions within a multivariate hydrological frequency analysis based on copulas (the second of which for sea storms). Bender et al. (2014) analysed the joint extremes of flood peak and flood discharge in Rhine River, introducing a multivariate nonstationary approach based on copulas. The latter study considered nonstationarity both in the marginal distributions of the variables involved and in their dependence structure. Jiang et al. (2015) also considered nonstationarity in the marginal distributions and/or the time variation in the dependence structure between different hydrological series to perform bivariate frequency analysis for the low-flow series from two neighbouring hydrological gauges using copulas. Kwon and Lall (2016) presented a nonstationary approach to assess the time-varying return period of the drought event of 2012–2015 in California based on the joint distribution of drought duration and severity modelled using copulas.

1.2 Scope of work

The destructive potential of marine storm events on coastal areas and structures depends critically upon storm surge, incident wave height and period for sea states with directional spreading that can affect the coast. The extremes of the aforementioned marine variables are controlled by synoptic atmospheric circulation patterns; thus, they usually show strong statistical dependence (Rueda et al. 2016). Wave periods have both deterministic and random links to wave height, delimited only by the potential energy content of a wave train or sea state. The former are mainly expressed in terms of physical limitations such as maximum wave steepness, while the latter are apparent as different combinations of wave height and period that may be produced from slightly a different meteorological forcing. Moreover, extreme wave conditions and large storm surges depend on the same driving force, the wind field; hence, dependence at extreme levels of the two processes is highly likely. The above-mentioned dependencies of marine variables and the fact that climate change is one of the prominent causes of long-term nonstationarities inherent in marine signals, especially when their extreme

levels are of interest, necessitate the use of a nonstationary multivariate approach to assess future extreme sea states that can provide reliable design values for the TWL at the shoreline and its variations with time.

In the present work, a nonstationary multivariate approach, partly based on the methodology presented by Bender et al. (2014), has been further extended and implemented to assess design TWL on the shoreline at selected Greek coastal areas in the Aegean Sea under the effects of climate change. The approach introduces different innovative features to estimating the elevation of TWL at the shoreline in the future climate (restricted to only one possible realisation of it), considering changes over time in all involved processes, both deterministic (MSL rise) and stochastic (variations in the marine climate), as well as in their associations. The use of modelled data for marine variables, forced by climate simulation results by an RCM, imposes the use of a fully nonstationary approach for modelling TWL, as such data exhibit time dependency in both their marginal distributions and their dependence functions. In this work, a bivariate EVA is conducted at two different spatial scales: one in the offshore area of selected coastal locations, which is quite common in joint probability analyses of marine variables, and another one in the nearshore area of these locations. The approach followed enables us to assess the dependence structure between the wave-induced sea level on the shoreline and the nearshore storm surge, considering that the modelled wave data are transferred from deep water to coastal areas. To do this, the well-established theory of Goda (2000) is implemented by an iterative modelling approach based on semi-analytic calculations of irregular wave propagation combined with semi-empirical graphical distributions of spectral wave parameters and constraints in the values of wave characteristics due to irregular wave breaking. The aforementioned bivariate analyses are performed for marine processes of similar nature, magnitude and spatial scales, i.e. for storm-driven and wave-induced water levels, as well as for offshore wave characteristics (significant wave height and peak spectral wave period). The nonstationary analysis of the present paper is also implemented based on strict directionality and duration constraints for both the storm wave and surge events. Comparing the core of the statistical methodology with the one presented in Bender et al. (2014), it should be noted that the present analysis also considers nonlinear trends in parameters of the marginal distributions and in the dependence parameters of the bivariate models and selects the best-fitted ones using different statistical criteria. Such trends are then incorporated in the bivariate copulas to produce joint return level estimates of both the offshore wave parameters and the nearshore water level components. Both Archimedean and Elliptical copulas are also included in the analysis, covering different forms and degrees of dependence at the two areas of application (offshore and nearshore).

In Sect. 2, the methodology to assess TWL at the shoreline is described including the transfer of wave data from deep water to shallow coastal areas and the estimation of the wave-induced sea level on the shoreline. Different study areas and datasets available for the analysis are also presented. Section 3 introduces the nonstationary generalised extreme value (GEV) distribution function and the copula theory, used to model the marginal distributions of offshore and nearshore marine variables and their dependencies, respectively. Section 4 includes the main results of the nonstationary analysis, while Sect. 5 summarises the main findings of the paper.

2 Estimation of total water level at the shoreline under the effects of climate change

Flooding of coastal areas is caused by the combined effect of high water levels (storm surges and astronomical tides), MSL rise and wave action of rough sea states. The wave-induced run-up at the shoreline has been calculated in the present work using the Stockdon et al. (2006) formula:

$$R_{2\%} = 1.1\left(0.35\tan\beta\left(H_s L_o\right)^{\frac{1}{2}} + \frac{\left(H_s L_o\left(0.563\tan^2\beta + 0.004\right)\right)^{\frac{1}{2}}}{2}\right)$$
$$R_{2\%} = 0.043\left(H_s L_o\right)^{\frac{1}{2}} \quad \xi < 0.3 \tag{1}$$

where H_s is the deep water significant wave height, L_o is the deep water wave length associated with the peak spectral wave period T_p, tanβ is the beach face slope and $\xi = m/(H_s/L_o)^{1/2}$ is the Iribarren number (surf similarity parameter). The formula of Stockdon et al. (2006) estimates run-up by adding wave set-up and swash and decomposes swash into the sum of incident and infragravity contributions. For dissipative beaches ($\xi < 0.3$), the wave run-up is infragravity dominated. It also takes into account the beach slope, indirectly incorporating the influence of morphological changes on the coast due to sediment transport erosion or accretion. As the latter was out of the scope of the present study, in the following methodology the beach morphology was not allowed to evolve; thus, tanβ is considered to be invariant. The TWL at the shoreline, η_t, resulted from adding the components of wave run-up (contains the wave set-up parameter, $\eta_{su,}$ and infragravity swash motions), $R_{2\%}$, MSL rise, MSLR, the surf beat, η_{sb}, the storm surge sea level height, SLH, and the highest astronomical tide, HAT (see definitions and details on values' ranges of all parameters in Sect. 2.1, 2.2):

$$\eta_t = R_{2\%} + \mathrm{MSLR} + \eta_{sb} + \mathrm{SLH} + \mathrm{HAT} \tag{2}$$

We added the surf beat component (although interrelated to infragravity bound long waves in the surf zone, parts of which are calculated in $R_{2\%}$) in the TWL calculation, in order to amplify the values of Stockdon et al. (2006) run-up parameter that do not take into account the swell-driven resonance with bound long waves in the surf zone and the correlated surf beat sea level elevations towards shoreline. Plant and Stockdon (2015) comment on the Stockdon et al. (2006) run-up model's inability to accommodate broad-banded or multiple peaks in the frequency or direction of wave spectra. The wave data used (see description in Sect. 2.2.2; Kapelonis et al. 2015) were based on SWAN model simulations in a coupled (pseudo-bimodal) swell/wind wave mode, rendering the extra surf beat term in the calculation of TWL, as a moveable breakpoint-generated sea level elevation induced by bichromatic/transient wave groups breaking on beaches (Baldock 2006; Baldock et al. 2000). In Eq. 2, reliable estimation of η_t depends significantly on purposeful choice of extreme values of wave-induced parameters ($R_{2\%}$, η_{sb}) and SLH. Thus, one of our goals was to constrain the estimation of SLH extremes in nearshore areas based on multivariate EVA of storm surges with wave-induced coastal sea levels, η_w. Full reasoning on the latter is given in the methodology presented in Sect. 3.

2.1 Methodology to transfer offshore marine data to nearshore areas

In order to correctly calculate the TWL in coastal areas, and specifically inside the surf zone and towards or on the shoreline (see also Sect. 3), we primarily need to transfer the spatially large-scale modelled (wave and storm surge) data from relatively deep (or intermediate) waters in the open sea to nearshore shallow water areas and finally the shoreline boundary. The storm surge is a rather large-scale phenomenon in the order of kilometres taking place on the continental shelf. Its effects, i.e. the storm-induced SLH, concern wide spatial scales and can be provided by dynamically downscaled numerical simulations in climatic mode (150 years) with adequate accuracy in terms of spatial resolution, e.g. 10–5 km in Mediterranean and Greek Climate Storm Surge (MeCSS and GreCSS) Models' implementations of Androulidakis et al. (2015) and Makris et al. (2015, 2016).

However, this might not be the case for the finer-scale effects of wave-induced sea level in nearshore areas and close to the shoreline, due to irregular wave breaking. To calculate the latter, very detailed, nested numerical simulations in climatic mode (150 years) with a 2-DH wave model of very fine spatial resolution would be required, which is currently a rather arduous or even impossible task in terms of computational resources or available detail of digital bathymetric and terrain models. Therefore, in the present work, in order to produce estimates of future extreme sea states, we have initially analysed extreme offshore wave characteristics, derived by numerical simulations of wave climate with the Simulating WAves Nearshore (SWAN) model (Kapelonis et al. 2015; Makris et al. 2016). Subsequently, we have calculated the transformation of the annual extremes of random wave characteristics (yearly extreme significant wave height, H_s; associated peak spectral period, T_p; related main wave propagation direction, a_p) towards the shoreline in specific sites of interest. An iterative modelling approach for irregular wave trains (Goda 2000; Makris and Krestenitis 2009) was implemented, taking into account the crude variations in the bathymetry crossing areas of nearshore intermediate to shallow waters. The model is based on blending spectral wave propagation and breaking, for wave fields crossing successive characteristic depths of marine areas, while dividing them in segments of rather parallel (and nearly straight) depth contours. The model is based on merging semi-analytical expressions with graphically derived semi-empirical distributions (Goda 2000) for wave variables linked to refraction and shoaling. The surf zone dynamics (wave breaking) is also taken into account by semi-analytical relations of depth-limited constraints for H_s in nearshore areas blended in the irregular wave propagation iterative calculation process. All the above is modelled in order to finally compute the spectral wave characteristics in the surf zone and result to a plausible estimation of the wave-induced water level on the shoreline, η_w.

The wave-induced set-up, η_{su}, was calculated (Goda 2000; Dean and Dalrymple 2002), as it represents the short- to midterm sea level elevation in the coastal zone, due to random wave action in shallow waters and secondary processes of irregular wave breaking. The former is added to another yet smaller component of sea level variation, known as the surf beat, which is a midterm oscillation of the sea level (with typical duration of more than 7–10 wave periods or several minutes) inside the surf zone with varying values from incipient wave breaking point to the shoreline (~ 30% of incident H_s). The surf beat, η_{sb}, is correlated with wave groups approaching the coastal zones in discrete high- and low-frequency bands, i.e. divided in groups of short and long waves, respectively. Conclusively, we estimated the (potential) wave-induced sea level,

$\eta_w = \eta_{su} + \eta_{sb}$, in the surf zone and on the shoreline (see Eq. 7 for semi-analytic relation for the evolution of the wave set-up in the surf zone and its asymptotic value exactly on the shoreline), being qualitatively similar to nearshore SLH due to storm surges, as they are both midterm (mean) sea levels of comparable magnitudes and of similar spatial scales, covering extended areas on beach fronts, and thus can be a fitting counterpart in a bivariate analysis of sea level values.

2.1.1 Transformation of random wave characteristics from open seas to shallow coastal waters

The spectral wave theory, semi-analytic relations and graphical wave parameter distributions of Goda (2000) were used for the propagation of irregular waves from deep or intermediate to shallow waters, by calculating the transformation of the spectral wave characteristics (H_s, T_p, a_p). Theory takes into account the physical processes of random wave propagation, refraction, shoaling and deformation of waves for the calculation of energy dissipation due to irregular wave breaking. Specifically, the modelling approach for the surf zone creation due to depth-limited breaking (Goda 2000) produces the random breaking wave characteristics considering the local bathymetry, the bottom slope and bottom friction.

The transfer of numerically simulated wave data from deep (bias-corrected values in selected cells of the SWAN computational grid; see also Sect. 2.2.2 and Makris et al. 2016) to coastal waters was based on Goda (2000), i.e. the derivation of the effective coefficients for random wave refraction and shoaling, k_r' and k_s', appropriately modified based on the classic k_r and k_s values from linear theory for monochromatic waves. The significant wave height, H_s, in arbitrary depth, d, is given by the relation $H_s = k_r' \cdot k_s' \cdot H_{s,o}$ (where the $_o$ index corresponds to offshore values). The areas of interest have been chosen to have rather parallel depth contours, and calculations were executed separately in consequent wave routes with rather straight depth contours, in order to preserve the applicability of the method. Energy dissipation due to breaking was calculated based on the marginal values of characteristic depths d_{30} and d_{50}, the angle of incidence of deep water waves, $\alpha_{p,o}$, the equivalent deep water wave concept $H_{s,o}' = k_s \cdot H_{s,o}$ for dealing with complex topographies and the spectral wave spreading parameter s_{max} for random waves.

The effective refraction coefficient for irregular waves is given by (Goda 2000):

$$\begin{aligned} k_r' &= f\left(k_r, h/L_{o,p}, a_{p,o}, s_{max}\right), && \text{from graphs} \\ k_r' &= \sqrt{\left[\sum_{i=1}^{M}\sum_{j=1}^{N}(\Delta E)_{ij}\left(k_r\right)_{ij}^2\right]}, && \text{analytically} \end{aligned} \tag{3}$$

where $k_r(f,\theta)$ is the linear refraction coefficient of a monochromatic wave component with frequency f and propagation direction θ, $(\Delta E)_{ij}$ are the components of relative wave energy with ith discrete frequency and jth angle of incidence for discrete spectral bands of random waves with $i = 1, M$ directional spreading range and $j = 1, N$ the frequency spreading range. The graphical way of deriving k_r' concerns coasts with rather straight and parallel depth contours and their pre-calculated values based on appropriate superposition methodology. Accordingly, the (effective) spectral shoaling coefficient for random waves is given by (Goda 2000):

$$\begin{aligned} k_s' &= k_s, && d_{30} \le d \\ k_s' &= \left(k_s\right)_{30} \cdot \left(\tfrac{d_{30}}{d}\right)^{2/7}, && d_{50} < d < d_{30} \\ k_s' &\cdot \left(\sqrt{k_s'} - B\right) - \Gamma = 0, && d < d_{50} \end{aligned} \tag{4}$$

where $L_{o,p}$ is the deep water wavelength corresponding to the peak spectral period, T_p, and the remaining parameters are given by (Goda 2000):

$$\left(\frac{d_{30}}{L_{o,p}}\right)^2 = \frac{2\pi}{30}\frac{H'_{s,o}}{L_{o,p}}(k_s)_{30}, \quad \left(\frac{d_{50}}{L_{o,p}}\right)^2 = \frac{2\pi}{50}\frac{H'_{s,o}}{L_{o,p}}(k_s)_{50}$$
$$B = \frac{2\sqrt{3}}{\sqrt{2\pi H'_{s,o}/L_{o,p}}}\frac{d}{L_{o,p}}, \quad \Gamma = \frac{C_{50}}{\sqrt{2\pi H'_{s,o}/L_{o,p}}}\left(\frac{L_{o,p}}{d}\right)^{3/2} \tag{5}$$
$$C_{50} = (k_s)_{50}\left(\frac{d_{50}}{L_{o,p}}\right)^{3/2}\left[\sqrt{(k_s)_{50}\cdot 2\pi H'_{s,o}/L_{o,p}} - 2\sqrt{3}\frac{d_{50}}{L_{o,p}}\right].$$

2.1.2 Calculation of wave-induced sea level on the shoreline

Deformation of random sea waves in nearshore areas, due to irregular wave breaking, plays the most important role in defining the wave-induced characteristics of the sea surface inside the surf zone. The energy dissipation due to depth-limited breaking of a random wave train that corresponds to a specific sea state, simulated by a third-generation wave model (SWAN; see also Sect. 2.2.2), can be computed analytically to produce a simple relation for the change of wave height distribution within the surf zone, based on the formulation of the limiting height of individual components of the breaking spectral waves, $H_{s,b}$ (Goda 2000):

$$H_{s,b} = A\cdot L_{o,p}\cdot\left\{1-\exp\left[-1.5\cdot\frac{\pi\cdot d_{s,b}}{L_{o,p}}\left(1+15\cdot m^{4/3}\right)\right]\right\} \tag{6}$$

where $A=0.12$–0.18 is a shape parameter depending on the position of the broken wave inside the surf zone, $d_{s,b}$ the incipient breaking depth corresponding to $H_{s,b}$ and m the bottom slope.

Combining iteratively the breaking model with the random wave transformation, one can calculate an estimation of the wave set-up evolution in the surf zone transverse to the coast, $d\eta/dx$ (variation in mean water level, being η_{su} exactly on the shoreline), together with the surf beat, η_{sb} (ζ_{rms} in Goda 2000). Adding the two aforementioned parameters, we can get the total sum of wave-induced sea level near or on the shoreline, $\eta_w=\eta_{su}+\eta_{sb}$ (Goda 2000; Dean and Dalrymple 2002):

$$\begin{aligned}\frac{d\eta}{dx} &= -\frac{1}{(\eta+d)}\cdot\frac{d}{dx}\left[\frac{1}{8}\overline{H_s}^2\left(\frac{1}{2}+\frac{4\pi d/L_p}{\sinh(4\pi d/L_p)}\right)\right], && \text{evolution inside the surf zone}\\ \eta_{su} &= \frac{3\gamma^2/8}{1+3\gamma^2/8}\cdot d_b - \frac{\gamma^2\cdot d_b}{16}, && \text{asymptotical value on the shoreline}\end{aligned} \tag{7}$$

$$\eta_{sb} \equiv \zeta_{rms} = \frac{0.01\cdot H'_{s,o}}{\sqrt{\frac{H'_{s,o}}{L_{o,p}}\left(1+\frac{d_{s,b}}{H'_{s,o}}\right)}} \tag{8}$$

where $\gamma = H_{s,b}/d_{s,b}$ is the wave breaking index, L_p the local wavelength corresponding to T_p and η the local value of the sea level (mean water level) due to the random breaking-induced process of the wave set-up in depth d.

2.2 Study areas and available datasets from high-resolution numerical models

2.2.1 Study areas

The methods and techniques of the present work have been implemented to the annual maxima of random wave characteristics (i.e. H_s and corresponding T_p) in open seas, nearshore wave-induced sea levels, η_w, and associated SLH values due to storm surges at selected locations of the Aegean Sea. Three representative study areas (Makris et al. 2016) have been selected (Fig. 1), one in the North Aegean (Area 1) containing the coastal zone of Alexandroupolis city and part of the Thracian Sea, one in the Central Aegean (Area 2) containing the coastal area of Eresos in the southern Lesvos Island and one in the South Aegean (Area 3) containing the coastal area of the city of Heraklion in northern Crete. As it is difficult to characterise or quantify a specific beach slope on standard rules (Coelho et al. 2009), we followed Short (1999) and adopted the beach slope between low tide

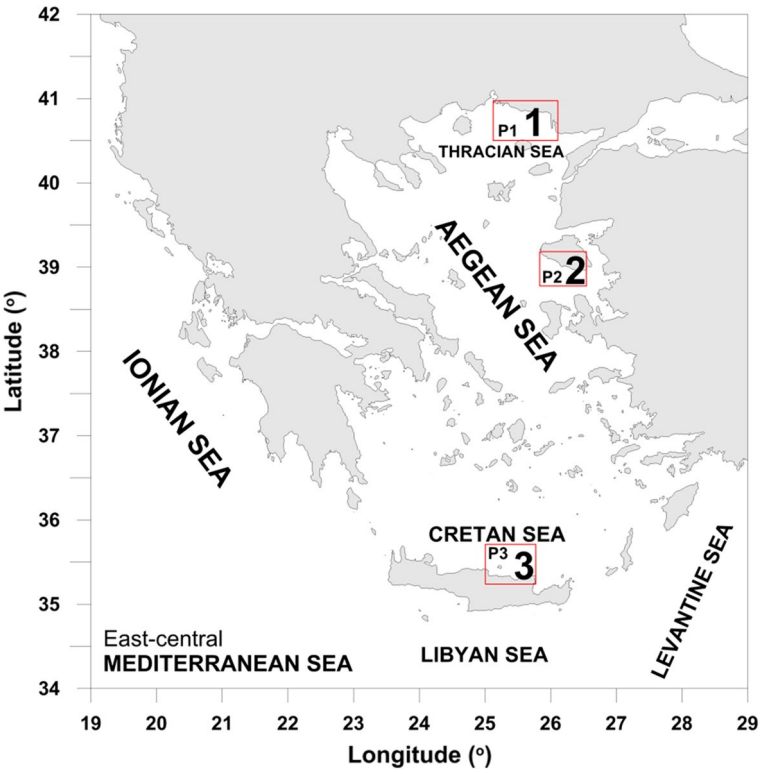

Fig. 1 Selected study Areas i ($i = 1$–3) of the Aegean Sea; 1: North Aegean, Alexandroupolis coastal area in the Thracian Sea; 2: Central Aegean, Eresos coastal area in southern Lesvos Island; 3: South Aegean, Heraklion coastal area in the Cretan Sea. P_i are characteristic grid points of the red boxes defining each Area, namely P1 [25.30°, 40.65°], P2 [25.75°, 39.00°] and P3 [25.15°, 35.70°], respectively

shoreline and the base of the sand dune for any location. The values were extracted from a Digital Elevation Model (DEM), freely provided from Greece's National Cadastre & Mapping Agency S.A. (http://www.ktimatologio.gr/sites/en/Pages/Default.aspx). The DEM's grid cell size was 5 m × 5 m, and correction field surveys and measurements were performed, where necessary. For the characterisation of each beach slope, an adequate number of representative cross-shore profiles were selected at each study area, namely 52, 5 and 18 beach slope profiles for Areas 1, 2 and 3, respectively. The discrete profiles were distanced 800–1000 m from each other. The chosen ones for the calculation of the run-up corresponded to the median values of each beach's series of profiles (e.g. ranging between 1 and 14% conclusively in all coasts). To isolate the influence of hydrodynamic forcing on TWL (Serafin et al. 2017), almost uniform (7‰ differences) beach face slopes were selected in all Areas considered. Thus, the representative beach profiles in Areas 1, 2 and 3 have beach slopes of almost 7.5%, 8.2% and 8%, respectively. The beach widths of the selected locations in Areas 1, 2 and 3 are 14 m, 21 m and 40 m, respectively, with corresponding berm heights of 3 m, 2 m and 3.2 m.

2.2.2 Available numerical data of wave and storm surge

The data concerning the marine parameters of the present work are drawn from long-term numerical simulations of 150 years, forced by atmospheric data produced by RCM climate simulations, to estimate the (offshore) wave characteristics (H_s and T_p) and the SLH due to storm surges at selected grid points of the study area. The nearshore (surf zone) wave-induced sea levels were derived based on the methodology given in Sect. 2.1.2, and the respective response on the coast, i.e. the TWL at the shoreline, is given in the start of Sect. 2. The wave data resulted from a wave climate modelling system, based on the SWAN model (Booij et al. 1999) formulated for the Mediterranean and the Aegean/Ionian Seas; for more information on exact numerical set-ups, thorough validations, and bias correction of wave characteristics, the reader is advised to follow the detailed descriptions of Kapelonis et al. (2015) and Makris et al. (2016). Storm surge simulations were based on high-resolution two-dimensional models of hydrodynamic ocean circulation (MeCSS, GreCSS Models), also formulated for the Mediterranean and Aegean/Ionian Seas at large (detailed model set-ups and validations can be found in Krestenitis et al. 2014; Androulidakis et al. 2015; Makris et al. 2015, 2016). The calibration and validation of the models were performed using in situ measurements from tide gauge stations and satellite altimetry observations. The modelled datasets covered a period of 150 years (1951–2100) and were produced within the research project "CCSEAWAVS (2012–2015): Estimating the effects of climate change on sea level and wave climate of the Greek seas, coastal vulnerability and safety of coastal and marine structures". The atmospheric forcing of the models consisted of simulated climatic data of wind and sea level pressure fields derived from an RCM, namely RegCM3 (Vagenas et al. 2014; Velikou et al. 2014). RegCM3 was built upon the NCAR—Pennsylvania State University (PSU) Mesoscale Model version 4 (MM4) (Dickinson et al. 1989). The spatial resolution of RegCM3 was 10 km × 10 km (Tolika et al. 2016), produced under 20C3M historical scenario for the twentieth century, and its future projections (twenty-first century) were forced by the output of a Global Climate Model (GCM), i.e. ECHAM5 (Roeckner et al. 2006) simulated fields, under the assumptions of the A1B emissions scenario (Makris et al. 2016; Vagenas et al. 2017). Tolika et al. (2016) and Makris et al. (2016) provide thorough validation of the dynamically downscaled RCM implementation against field observations and ERA-Interim atmospheric re-analysis data

(http://www.ecmwf.int/en/research/climate-reanalysis/era-interim), together with all the special features of numerical set-up for regional-scale future climatic projections. Their goal was to focus on the potentials of well-validated dynamical downscaling for the aid of climate estimations and not on ensembles of future scenarios based on multiple parent GCMs. This was associated with an effort to reduce the obvious high uncertainty of extreme future climate estimations, which was induced by the use of a unique GCM-scenario combination.

2.2.3 Selection of representative grid points and definition of storm events

The selection of representative points of the wave and storm surge models' grids has been performed utilising the homogeneity measures of Hosking and Wallis (1997). In the present work, homogeneity measures were assessed based on annual maxima of H_s and SLH for the control (1951–2000) and the future (2001–2100) periods, and homogeneous regions in terms of the extreme marine climate were defined (Makris et al. 2016). It should be noted that the study areas were judged to be acceptably homogeneous regarding extreme SLH. The methodology of the present paper has been applied to one representative grid point per study area, belonging to the homogeneous group with the highest wave height quantiles; therefore, P_i are the characteristic grid points of each Area i ($i=1$, 3; 1: North Aegean, 2: Central Aegean, 3: South Aegean in Fig. 1) with P1 [25.30°, 40.65°], P2 [25.75°, 39.00°] and P3 [25.15°, 35.70°], respectively.

The Aegean Sea is a semi-enclosed water basin labelled as a marginal sea (bordering continents semi-isolated from huge water bodies and open oceans usually confined by island arcs or lands, e.g. the Cyclades, Crete etc.). For such a reason, there are no immense water masses (as in oceanic waters) to drive very high storm surges in the coastal zone. Moreover, storm surge events in the Aegean are usually generated by enfeebled subtropical cyclones and/or extra-tropical storms that follow a west-to-east path over the Mediterranean Sea (Krestenitis et al. 2011; Makris et al. 2016). Therefore, flooding of Greek coastal areas is more influenced by the wave action. Based on the aforementioned peculiarities of the study area and the fact that wave periods are usually strongly dependent on and physically constrained by wave height, we decided to select our multivariate storm events based on annual maximum offshore wave heights of directions affecting the coastal areas under study and exceeding a minimum duration to be able to cause significant impact on the coast. These multivariate sea states can provide the highest possible realisations of TWL in the area, contributing to the most severe flooding hazard.

Wave height events exceeding appropriately defined thresholds, ranging between 1.5 and 2 m in all study areas for durations of more than 6 h, were initially selected at all considered grid points. The main offshore direction θ_p of irregular wave propagation (direction normal to wave crest of each spectral component) was produced by the SWAN model simulations in Cartesian convention (taken counterclockwise from geographic East), and it was transformed for every case to $a_p \leq \pm 90°$ in order fit the spectral wave direction limit of the Goda (2000) modelling approach. Thus, the total aperture of wave propagation was taken to be 160° (including almost all oblique incident wave fields towards the shoreline), i.e. giving an 80° maximum initial angle of propagation on each side of the transverse to the coastline of each studied area. The H_s annual maxima of the defined events and associated T_p values were then selected at all grid points, corresponding to a period of 150 years (1951–2100). The lower spatiotemporal variability of the intensity of storm surges compared to rough wave fields in the Aegean Sea allowed us to use the (lower-resolution)

modelled, nearshore, storm-driven SLH that corresponds to the respective annual maxima of H_s. In this framework, not only the simultaneous, but a 5-day window of SLH data were implemented in the analysis, covering the time of corresponding records of H_s maxima (by 2.5 days bilaterally), in order to estimate the largest possible SLH response to the particular storm events, which usually have a maximum duration of 120 h in the Mediterranean basin (Conte and Lionello 2013; Makris et al. 2016). Please note that the nearshore wave-induced water levels, η_w, are computed using only these annual maxima pairs of H_s and T_p in order to transfer offshore yearly extremes to the shoreline, following the reasoning presented in Sect. 2.1. The proposed selection method for extreme offshore conditions ensures the capturing of almost the entire sample space of H_s–T_p pairs that could drive extreme flooding events. Some pairs of longer but shorter waves that could theoretically drive larger flooding might exist (yet statistically insignificant, i.e. with occurrence probability < 5%), but furthermore do not necessarily qualify as efficient wave storm events, either because of their insufficient short duration (< 6 h) or ineffective directionality (incident waves away from the impact shoreline).

2.2.4 Mean sea level rise and tidal components

To assess the MSL rise in the Aegean Sea used in Eq. 2, both a steric component and a component of mass addition due to ice melting were considered in this paper. The estimate used for the steric contribution was based on the projected thermosteric sea level rise (SLR) of about 5 cm for the Aegean and Ionian Seas by 2050 (vs. 1951–2000) under the SRES-A1B scenario (Carillo et al. 2012). Other components of MSL rise (e.g. mass addition due to land ice melting) were also considered by adding 15 cm to the thermosteric component, according to the IPCC AR5 (IPCC 2013). The total value of MSL rise for the Aegean Sea used in this work, namely 25 cm by 2100, agrees well with recent estimates of MSL trend due to changes in the mass (GRACE programme), corresponding to about 2.5 mm/year, averaged over the whole Mediterranean for the period from January 2003 to July 2013 (Tsimplis et al. 2013). If this trend remains constant, the mass addition should raise the Mediterranean MSL by approximately 12 cm by 2050 and 25 cm by 2100 (Makris et al. 2016). The range of highs and lows of astronomical tides in the Aegean, and especially in the areas of interest, are generally small compared to other European coastal areas (Pugh 1996). The approximation of the largest HAT value in the three specific areas of the Aegean basin is taken equal to 25 cm, courtesy of Hellenic Navy Hydrographic Service (https://www.hnhs.gr/en/), based on the works of Tsimplis (1994) and Tsimplis et al. (1995).

3 Methodology for nonstationary analysis of extreme marine events

Our basic intent was to perform analysis of extremes based on bivariate distributions of marine variables (viz. η_w and SLH) and nonstationary GEV functions of nearshore data in coastal areas, instead of statistically correlating offshore values of wave and surge parameters and then applying the derived extremes in coastal areas. The main goal was to constrain the choice of surge-induced SLH extremes based on multivariate analysis with wave-induced coastal sea levels. As aforementioned, the nearshore data that we have used are numerically modelled results of SLH (MeCSS and GreCSS Models one-way coupled simulations of 150 years) and wave characteristics (H_s, T_p, a_p) by two case-specific SWAN

implementations with nested grids in the Mediterranean and the Aegean and Ionian Seas for 150 years, complemented by a requisite, simplistic model for irregular wave propagation and breaking in nearshore areas and shallow waters towards the shoreline.

Therefore, we tried to ensure that the cases of extreme waves (taking into account nearshore processes as spectral wave refraction, shoaling and breaking) are combined with extreme surges in shallow coastal areas, in order to finally define TWL on the shoreline which actually refer to extreme cases that really pose flooding threats on the coast. We approached the later through bivariate analysis of drivers, as the past literature has focused on bivariate EVA of offshore surge and wave parameters or univariate EVA on the response (wave run-up or TWL). Moreover, we performed bivariate analysis of extremes on uniform parameters, i.e. nearshore (and not offshore) SLH (due to storm surges) and n_w (wave-induced sea level), being of comparable magnitudes and similar spatial scales (they both cover extended areas on beach fronts), instead of correlating H_s or T_p to SLH (i.e. different types of parameters). Conclusively, the Stockdon et al. (2006) formula for $R_{2\%}$ was implemented in the end, as it is the most recent established approach on run-up calculation including both wave set-up and swash, but only after the more unambiguous estimations of return values of SLH and wave characteristics, to finally define plausible values of TWL. Please note that η_w was calculated by a numerically modelled approach throughout the surf zone ($d\eta/dx$ in Eq. 7), while $R_{2\%}$ is a statistical empirical estimation of the water level on the coast (considerably depending on the swash), and thus, its calculation relies much on the geometry of the beach face slope (especially for long waves which are mostly responsible for coastal inundation). Hence, bivariate EVA is performed for a pair of (modelled) physical parameters, viz. SLH and η_w, instead of a couple consisting of physical (SLH) and empirical ($R_{2\%}$) parameters; η_w is explicitly included in the end of the calculation process in $R_{2\%}$ (see start of Sect. 2). To sum up, our approach is based on applying bivariate extreme analysis on the drivers (storm surges and waves) of sea level elevation in broad nearshore areas, in order to define non-evasive cases of extreme water levels, avoiding mere univariate EVA on response parameters of sea level elevation on the coast (viz. TWL).

3.1 The GEV distribution function

The univariate EVT includes models for block maxima and models for exceedances over appropriately defined thresholds (POT models). The former correspond to the GEV distribution function, which is a three-parameter distribution, including the location, μ, the scale, $\sigma>0$, and the shape, $\xi\neq0$, parameters. The special case with $\xi=0$ corresponds to the Gumbel distribution function. The parameters of the GEV distribution function can be assessed using different estimation methods. Among them, the Maximum Likelihood Estimation (MLE) procedure is very commonly used and is quite easy to apply. However, the method of L-moments (LM) introduced by Hosking (1990) has been identified in the literature as more reliable and robust, even for relatively small sample sizes. The L-moments are analogous to ordinary moments and can be computed from linear combinations of probability weighted moments. In fact, they provide measures of the basic aspects of the shape of distributions or data samples, such as location, dispersion, skewness and kurtosis. Exact formulas for the Cumulative Distribution Function (CDF) of the GEV, the probability weighted moments and their applications are provided by van Gelder (1999) and Galiatsatou and Prinos (2016).

Most marine variables, especially at their extreme levels, exhibit phenomena of nonstationarity. Natural climatic variability and climate change are some of the prominent causes

of such nonstationarities. Natural climatic variability is mainly associated with internal interactions between components of the climate system. Such components are, among others, the El Niño Southern Oscillation (ENSO), the Pacific Decadal Oscillation (PDO) and the North Atlantic Oscillation (NAO), acting on different time scales. The aforementioned oscillations can have a significant impact on the magnitude of extreme marine events and on the occurrence of flood events. Climate change, with strong evidence existing nowadays on its existence and impacts, is associated in the literature with extreme events of higher intensity and frequency. Therefore, climate change can also be considered as a major cause of nonstationarity of marine extremes. The aforementioned causes contribute significantly to the nonstationary behaviour of extreme marine events and necessitate to incorporate time -varying components in the EV models, for the process of extrapolation to be more reliable and unbiased. To incorporate nonstationarity in modelling the univariate extremes of a marine variable, the three parameters of the GEV are assumed to vary as functions of time. Therefore, the nonstationary version of the GEV becomes (Coles 2001):

$$G(x) = \exp\left[-\left\{1 + \xi(t)\frac{(x-\mu(t))}{\sigma(t)}\right\}^{-1/\xi(t)}\right], \quad 1 + \xi(t)\frac{(x\text{ - }\mu(t))}{\sigma(t)} > 0 \tag{9}$$

Return levels x_p corresponding to return periods of T (years) $= 1/p$ are assessed as a function of time representing the quantile of the distribution function of the studied variable in a given year (Galiatsatou and Prinos 2016). To estimate the parameters of the fitted theoretical distribution functions of all the studied marine variables, the methodology presented in Bender et al. (2014) was implemented in the present work. A moving time window of 40 years length was shifted by 1 year each time, and the parameters μ, σ and ξ were estimated using the LM method for each time period. The parameter estimates extracted, using the above-mentioned procedure, correspond to the last year of each 40-year period (moving window). The time window length has been selected to meet two basic requirements (Bender et al. 2014): (1) its length should be selected short enough for the assumption of stationarity to be quite sound and adequate for the fitting of EV models, and (2) the data set of each time window should be large enough to provide a good fit of the marginal distributions of the marine variables as well as of their possible dependence structure. Stationarity of all moving windows was checked using different nonparametric trend tests, such as the Mann–Kendall trend test (Hipel and McLeod 2005), the Cox–Stuart trend test (Rutkowska 2015) and the Wald–Wolfowitz test (Rai et al. 2013) for independence and stationarity. The three aforementioned nonparametric trend tests were performed for the selected extremes of each marine variable in all 40-year moving windows and for all the three coastal areas considered (North, Central and South Aegean Seas). Very few datasets (selected H_s, T_p, η_w and SLH events) did not pass the three tests at a 5% significance level, and still all calculated failures were marginal; therefore, it was assumed that the condition of stationarity is satisfied for all moving windows.

3.2 Modelling dependence using copulas

In a multivariate framework, nonstationarity can emerge in the statistical attributes of the univariate variables, in the dependence structure of these variables, or both. Coastal flooding or failure of a coastal defence system depends critically upon crucial combinations of incident wave heights with directions towards the coastal area, incident wave (peak spectral) periods and SLH due to storm surge, viz. factors being interdependent, especially at their extreme

levels. Therefore, extraction of nonstationary marginal distribution functions for all marine variables (Sect. 3) has to be followed by a nonstationary joint probability analysis of the dependent variables using bivariate copulas. The main advantage of copulas over other multivariate distributions hinges on the fact that the dependence structure of the variables can be modelled independently from their marginal distributions. Copulas are multivariate distribution functions with uniform margins over (0, 1). If X_1 and X_2 are random variables with continuous marginal distributions $u_1 = P(X_1 \leq x_1)$ and $u_2 = P(X_2 \leq x_2)$ defined on the unit cube $[(u_1, u_2) \in (0, 1)^2]$, a copula can be defined as (Nelsen 2006):

$$C(u_1, u_2) = \Pr\left(U_1 \leq u_1, U_2 \leq u_2\right) \tag{10}$$

In the present work, three one-parameter Archimedean copulas based on a generator φ (Bender et al. 2014) have been utilised, namely the Clayton, the Frank and the Gumbel. The former is characterised by strong lower tail dependence, the middle one by weak tail dependence and the latter by strong upper tail and weak lower tail dependence. For the above-mentioned Archimedean copulas, the copula function $C(u_1, u_2)$ can be, respectively, given by (Bender et al. 2014):

$$\begin{aligned} C_{\text{clayton}}(u_1, u_2) &= \left(u_1^{-a} + u_2^{-a} - 1\right)^{-(1/a)} \\ C_{\text{frank}}(u_1, u_2) &= -\frac{1}{a} \ln\left[1 + \frac{(e^{-a \cdot u_1} - 1)(e^{-a \cdot u_2} - 1)}{e^{-a} - 1}\right] \\ C_{\text{gumbel}}(u_1, u_2) &= \exp\left\{-\left[\left(-\ln u_1\right)^a + \left(-\ln u_2\right)^a\right]^{1/a}\right\} \end{aligned} \tag{11}$$

The dependence parameter a ranges in the intervals $(0, \infty)$ for the Clayton, $-\ln(-\infty, \infty)/\{0\}$ for the Frank and $[1, \infty)$ for the Gumbel copulas. The Gumbel and the Clayton copulas represent only the case of independent and positive dependent variables, while the Frank represents the maximum range of dependence allowing both positive and negative dependence in the data. In the present work, the dependence parameter of the copulas has been assumed to vary with time, $a(t)$.

Apart from the one-parameter Archimedean copulas, two Elliptical copulas were also implemented in the present work, namely the bivariate Student's t-copula and the bivariate Gaussian copula. The bivariate Student's t-copula function $C(u_1, u_2)$ can be given by (De Kort 2007):

$$C_t(u_1, u_2) = t_{v,a}\left(t_v^{-1}(u_1), t_v^{-1}(u_2)\right) \tag{12}$$

where $t_{v,a}$, with $a \in [0, 1]$ and v the degrees of freedom, is the bivariate distribution corresponding to the univariate t-Student distribution, t_v (De Kort 2007). The generator for the Student's t-copula is regularly varying, and the copula has tail dependence for all $v > 0$. The degrees of freedom of the Student's t-copula were considered fixed in the present work ($df = 4$). The Student's t-copula converges to the Gaussian copula, when the degrees of freedom tend to infinity. The bivariate Gaussian copula function $C(u_1, u_2)$ is given by De Kort (2007) and presented in Galiatsatou et al. (2016). The dependence parameters of the two Elliptical copulas were also considered to vary with time, $a(t)$.

To estimate the dependence parameter of the copula functions, Joe and Xu (1996) proposed a two-stage procedure known as inference functions for margins (IFM). The marginal parameters, θ, are first estimated:

$$\hat{\theta}_{\mathrm{IFM}} = \arg\max_{\theta} \sum_{i=1}^{n} \sum_{j=1}^{p} \log f_j\left(X_{ij};\theta\right) \tag{13}$$

where $i = 1,\ldots n$ the number of independent realisations from a multivariate distribution and $j = 1,\ldots, p$ the number of margins with probability density f_j. Then, the dependence parameter of a multivariate copula is estimated given the marginal parameters (Yan 2007):

$$\hat{a}_{\mathrm{IFM}} = \arg\max_{a} \sum_{i=1}^{n} \log c\left(F_1\left(X_{i1};\hat{\theta}_{\mathrm{IFM}}\right), F_2\left(X_{i2};\hat{\theta}_{\mathrm{IFM}}\right), \ldots, F_{\mathrm{P}}\left(X_{\mathrm{ip}};\hat{\theta}_{\mathrm{IFM}}\right);a\right) \tag{14}$$

When each marginal CDF has its own parameters θ_j, the first step of the IFM procedure consists of a ML estimation for each $j = 1, \ldots, p$ (Yan 2007):

$$\hat{\theta}_{j\mathrm{IFM}} = \arg\max_{\theta_j} \sum_{i=1}^{n} \log f_j\left(X_{ij};\theta_j\right) \tag{15}$$

When a consistent estimation of the dependence parameter a is of importance, the Canonical Maximum Likelihood (CML) method can be utilised, without first specifying the marginal distributions. In case of a bivariate copula, the marginals are first transformed to pseudo-observations with uniform margins $(U_{i1}, U_{i2})^{\mathrm{T}}$ using the empirical CDF of each marginal distribution:

$$U_{i1} = \frac{R_{i1}}{(n+1)} \quad \text{and} \quad U_{i2} = \frac{R_{i2}}{(n+1)} \tag{16}$$

where R_{i1} and R_{i2} represent the ranks of X_{i1} and X_{i2}, respectively, n is the number of bivariate pairs and then the dependence parameter, a, is estimated as (Yan 2007):

$$\hat{a}_{\mathrm{CML}} = \operatorname*{argmax}_{a} \sum_{i=1}^{n} \log c(U_{i1}, U_{i2};a) \tag{17}$$

To select an appropriate copula function among the five presented above (Clayton, Frank, Gumbel, Student's t and Gaussian copula), the parametric bootstrap procedure proposed by Genest et al. (2009) has been utilised. The test computes the Cramér–von Mises functional S_{n}, comparing the empirical copula of the observations with a parametric estimate of the copula derived under the null hypothesis. Approximate p values for the test have been computed using the parametric bootstrap procedure. Large values of S_{n} usually result in the rejection of the null hypothesis that the bivariate data result from the tested copula function.

To estimate the dependence structure of the data within the introduced nonstationarity framework, the 40-year moving windows, utilised to estimate the marginal parameters of the studied marine variables, have been also applied to the bivariate data. Pseudo-observations of the dependent variables were first extracted. The dependence parameters for all selected copula functions were then calculated for each moving window using the CML procedure of Eq. 17. After estimating the copula parameters, the statistic S_{n} and its associated p values were assessed for all moving windows and all candidate copula functions. For each bivariate pair, the copula that resulted in p values

exceeding the 5% significance level for the entire study period was selected as the best-fitted model and applied for joint exceedance probability estimation. In case more than one of the fitted copulas satisfied the above condition, the selected bivariate model was the one providing the lowest Akaike Information Criterion (AIC) values during the largest part of the studied time interval (Akaike 1974).

In the framework of multivariate statistics, the joint return period can be estimated from the joint exceedance probability of a pair of events as in Galiatsatou and Prinos (2016).

The implementation of multivariate EV models results in an infinite number of combinations of the variables involved corresponding to each joint return period. Therefore, for a given joint exceedance probability, an infinite number of combinations of the dependent variables can be equally selected to be used in the design process. To overcome the selection problem, Salvadori et al. (2011) presented the most likely design event method. This method identifies the multivariate event with the highest joint probability density, among events belonging to the same joint exceedance probability isoline (Gräler et al. 2013):

$$\left(u_1, u_2\right) = \underset{T_{X_1 X_2}}{\arg\max} f_{X_1 X_2}\left(F_1^{-1}\left(u_1\right), F_2^{-1}\left(u_2\right)\right) \tag{18}$$

The resulting design values (x_1, x_2) can then be estimated using the inverse of the CDFs of the marginals (Galiatsatou and Prinos 2016).

The wave-induced run-up has been estimated by means of Eq. 1 as a function of the most likely design events of offshore H_s and T_p, while estimates of the most likely design events of nearshore SLH and wave-induced sea level on the shoreline, η_w, were also considered as different components of the η_t process. It should be noted that since the wave set-up is already included in $R_{2\%}$, only the surf beat component was added to the other water level components, estimated as a certain proportion of the most likely design event of η_w at each area under study.

4 Nonstationary analysis of the offshore and nearshore marine variables

4.1 Estimation of the marginal distributions

Annual maxima H_s of incident onshore waves (see Sect. 2.2.3) and the corresponding T_p values in deep water as well as simultaneous estimates of η_w and maximum SLH at selected nearshore areas have been processed using a moving time window of 40 years length for fitting EV models and identifying dependence structure of bivariate data (H_s–T_p and η_w–SLH). The GEV distribution was fitted to all time windows of all four studied marine variables. The goodness of fit of the GEV distribution function has been checked by means of the Kolmogorov–Smirnov test, and the model was identified to be suitable (p values were estimated higher than the 5% significance level for all moving windows). It should be noted that the GEV has been selected among other candidate theoretical models (i.e. the Normal, the Log-Normal and the Gamma) as the best-fitted one for all studied variables in both offshore and nearshore areas of the Aegean Sea, by means of goodness of fit tests and minimisation of root mean square error (RMSE) between data and respective quantiles estimated by the theoretical models.

The extracted time-dependent GEV parameters (μ, σ, ξ) from all the 40-year moving windows for annual maxima of H_s and corresponding T_p in Area 1 (North Aegean) are

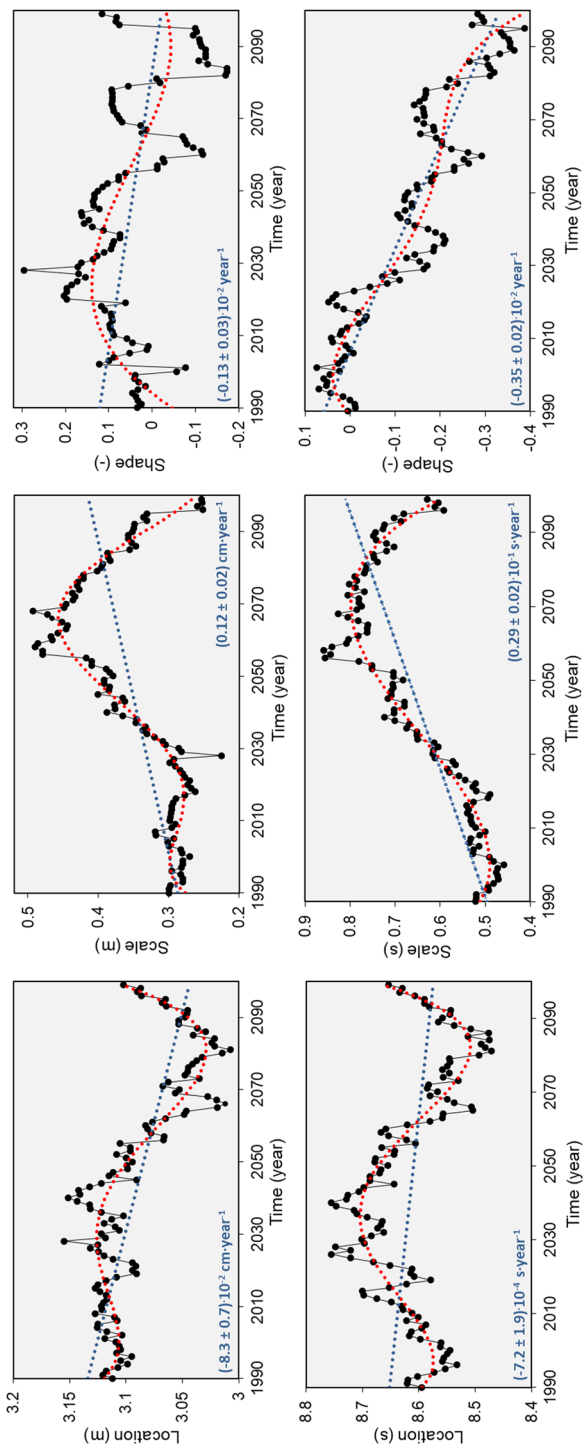

Fig. 2 Time-dependent series of location, μ (first column), scale, σ (second column), and shape, ξ (third column), GEV parameters for H_s (first row) and T_p (second row) at Area 1 (North Aegean Sea). Black dotted lines correspond to estimates from the 40-year moving windows; dashed blue and red lines represent statistically significant linear and polynomial trends (5% significance level), respectively. Values of linear trends (mean ± standard errors) are also given in the graphs

presented in Fig. 2; similar plots were also produced for Areas 2 and 3 (Central and South Aegean, respectively; not presented here for the sake of brevity). The ordinary least squares method has been utilised to fit linear and polynomial trends to all GEV parameter estimates. The significance of linear trends has been assessed using the Mann–Kendall test (Hipel and McLeod 2005), while the statistical significance of polynomial terms has been judged using the t test (Chambers 1992). An analysis of variance (ANOVA) was then utilised to compare between trend models with statistically significant polynomial terms (5% significance level), to identify the simplest one that can provide an adequate description of the inherent trend in the GEV parameters.

For all areas considered, statistically significant linear trends have been detected in all GEV parameters for both H_s and T_p. More specifically, for Areas 1 and 2 (North and Central Aegean), the statistically significant linear trends detected in the two offshore variables reveal similarities in their evolution over time. Extreme offshore wave characteristics at Area 1 are fitted to distribution functions with progressively lower means (in the future than in the past), higher variances and lighter tails, which can be attributed to the decreased relative contribution of severe zonal wind components to the generation of extreme wave heights in the second half of the twenty-first century, as shown by Galiatsatou et al. (2016) in their GEV-CDN (Conditional Density Network) model results with Principal Component Analysis (PCA) covariates of wind drivers. In Area 2, the GEV distribution functions present lower mean values and variances (in the future than in the past), but heavier tails arise in the future, possibly attributed to the rise of Etesians (i.e. local strong meridional winds called "Meltemia"; Maheras 1980) and their tendency to sidetrack towards the central part of the Aegean. For Area 3 (South Aegean), linear trends identified in H_s are of opposite sign to those in T_p, revealing discordance in the evolution of the two variables with time. The existence of a dense island cluster (Cyclades) may be responsible for this effect, due to diffraction of long waves having prominent impacts on H_s extremes. This is partly corroborated by Galiatsatou et al. (2016) that showed insignificant changes in extreme H_s magnitudes, notwithstanding the directional shift of driving wind fields from the first to the second half of the twenty-first century (Anagnostopoulou et al. 2014).

The former rationale also applies on the results of the ANOVA revealing the existence of statistically significant polynomial trends in all GEV parameters of the two offshore variables. In almost all GEV parameters, such polynomial trends are of order higher than three, identifying quite high variability in their estimates with time. Most best-fitted polynomial trends in the location parameter, μ, of H_s and T_p are of fourth order, revealing quite a homogeneous behaviour in the variation in mean values of extreme wave parameters in the Aegean Sea. However, larger differences are observed in the variations in the scale and the shape GEV parameters of H_s and T_p. The scale, σ, which shrinks or stretches the distribution of offshore wave parameters, and the shape, ξ, which distinguishes the distribution type and dictates the limiting behaviour of the GEV, are best-fitted by fifth-order polynomial trends at Area 2, revealing considerable variability in the respective estimates of H_s and T_p return levels. Statistically significant fifth-order polynomial trends are also detected in the scale and in the shape parameter of H_s at Areas 1 and 3, respectively. In general, larger variability, represented by higher-order polynomial trends in the GEV scale and shape parameters, is detected in H_s extremes, while lower -order polynomial trends are detected in the GEV parameters of T_p, especially at Area 3 in the south Aegean Sea (second-order and third-order polynomial trends are detected for the scale and shape parameters, respectively). Therefore, the variability in extreme T_p seems to be less pronounced compared to H_s, possibly attributed to the combination of multiple changes in

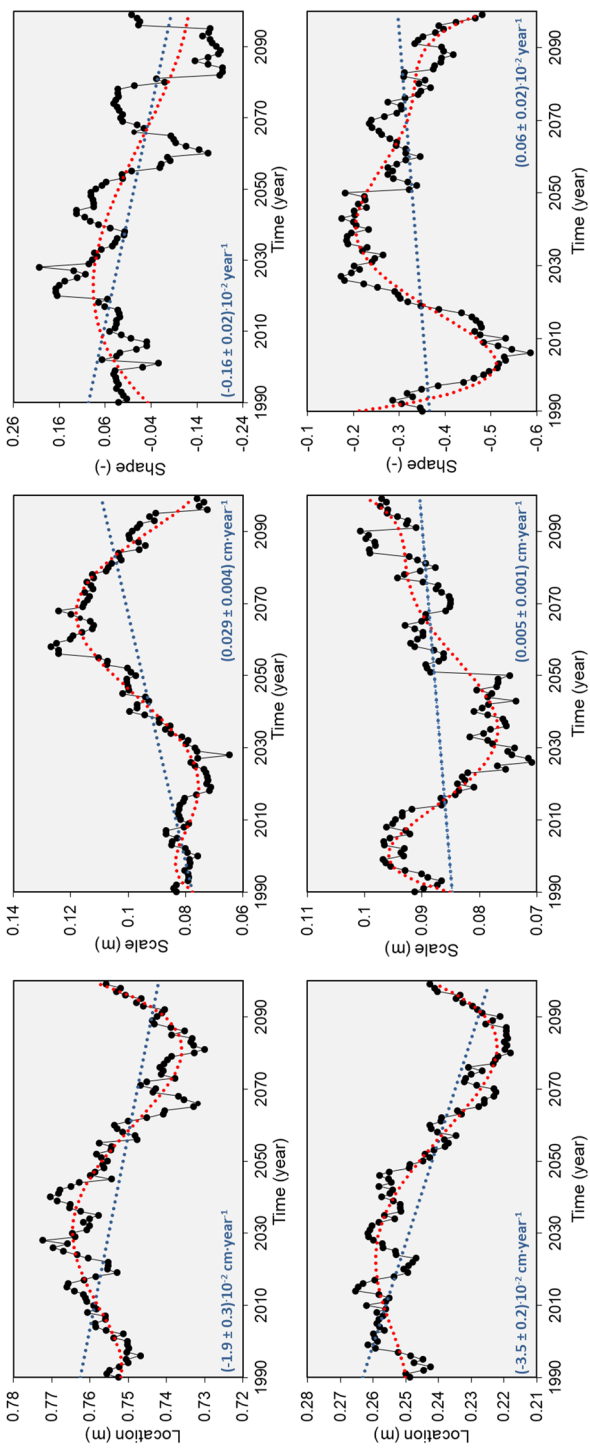

Fig. 3 Time-dependent series of location (first column), scale (second column) and shape (third column) parameters of the GEV for η_w (first row) and SLH (second row) at Area 1 (North Aegean Sea). Black dotted lines correspond to estimates from the 40-year moving windows; dashed blue and red lines represent statistically significant linear and polynomial trends (5% significance level), respectively. Values of linear trends (mean ± standard errors) are also given in the graphs

wind patterns throughout the twenty-first century (Anagnostopoulou et al. 2014) and the semi-confined water basin of the Aegean with many fetch-limited areas in it.

Figure 3 presents the respective time-dependent GEV parameter estimates for the two nearshore variables at Area 1, the wave-induced sea level on the shoreline (η_w) and the respective maximum storm surge (SLH). In all studied nearshore areas (results for Areas 2 and 3 are not shown here for the sake of brevity), statistically significant linear and best-fitted polynomial trends in the GEV parameters of η_w are similar to those extracted for the offshore H_s, as expected. Statistically significant linear trends exist in almost all GEV parameters for SLH. Linear trends in SLH, offshore H_s and η_w at each selected location are in accordance with each other, revealing similarities in the evolution of their extremes with time, possibly caused by the evolution of the extreme wind regime. The ANOVA reveals high (i.e. fourth and fifth)-order polynomials in all GEV parameters for SLH, presenting high variability in the mean, the variance and the tail behaviour of the extreme SLH distributions. This can be possibly attributed to the variations in the synoptic scale patterns, viz. storm-related sea level pressure (SLP) fields driving SLH extremes (inverse barometer effect). In general, there is apparent intense variability in every statistical parameter of the GEV for all marine variables.

4.2 Estimation of the dependence structure of the marine variables

After estimating the marginal distributions of offshore and nearshore variables, copula functions have been fitted to the pseudo-observations of the bivariate pairs of H_s–T_p and η_w–SLH, of the 40-year moving windows. The fitted copulas were the one-parameter Archimedean (Clayton, Frank, Gumbel), the Student's t with four degrees of freedom ($df = 4$) and the Gaussian. The goodness of fit test of Genest et al. (2009) has been applied to select the best-fitted copula (Sect. 3.2) among the different candidate bivariate models. Based on the aforementioned goodness of fit test, only the dependence functions giving p values higher than the 5% significance level during the entire interval of study (1990–2100) were considered. In cases where more than one of the studied copulas satisfied this constraint, the one that gave the lowest values of the AIC for the largest part of the study period was selected. Figure 4 presents results of the parametric bootstrap goodness of fit test for the pair of offshore (H_s–T_p) and nearshore (η_w–SLH) variables at Area 1.

The Gumbel copula, characterised by strong upper and weak lower tail dependence, has been selected to model the dependence structure of both bivariate pairs of offshore and nearshore variables in Area 1. The above-mentioned conditions (low S_n values with p values > 5%) are satisfied for the entire interval of study. The Gumbel copula has also been selected as the best-fitted model for the dependence function of offshore H_s and T_p in Area 2, identifying strong upper tail dependence of the two wave parameters. Conditions are also met for all time steps, while having the lowest AIC values for the largest part of the interval 1990–2100, compared to all other candidate copulas. Strong upper tail dependence of H_s and T_p, observed in the North and Central Aegean Sea areas, is not apparent for Area 3 (South Aegean), where the Frank copula prevailed, identifying weak tail dependence of H_s–T_p extremes, though detecting quite strong dependence for the remaining part of the extremal distributions. Fetch-limited conditions of wind wave generation in the southern parts of the Aegean are possibly responsible for limiting upper tail dependence of H_s–T_p. Considering the pair of nearshore variables, the Gaussian copula has been selected as the best-fitted bivariate model for Areas 2 and 3. The Gaussian copula, characterised by the absence of tail dependency, was the only bivariate model with p values higher than 5%

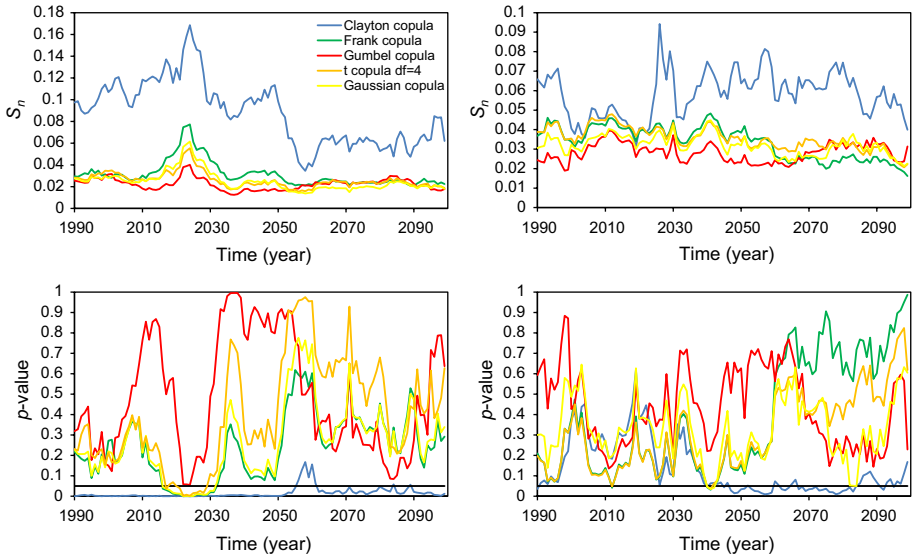

Fig. 4 Parametric goodness of fit results for the dependence structure of offshore H_s–T_p (first column) and nearshore η_w–SLH (second column) at Area 1 in the North Aegean Sea. The upper panel (first row) shows results of the statistic S_n for different copulas. The lower panel (second row) shows the corresponding p values also including the 5% significance level (black line)

significance level for all time steps, while showing the lowest AIC values during the entire period 1990–2100.

After selecting an appropriate copula function, the dependence structure of all offshore and nearshore variables has been fitted to the bivariate pseudo-observations of each moving 40-year window and the dependence parameter of each copula has been calculated. Figure 5 presents the time-dependent parameters of all selected copula functions in each study area. Statistically significant linear trends can be detected in almost all dependence parameters, except from the one characterising the dependence function of the nearshore pair of η_w and SLH in the South Aegean Sea (Area 3). Detected linear trends are all negative for the dependence function of the offshore wave parameters, showing a decrease in monotonic dependence of the two variables with time, while linear trends appear in Area 1 for η_w and SLH. Considering the selected best-fitted polynomial trends, a statistically significant concave trend has been detected in the dependence parameter of the Gumbel and Frank copula for the offshore H_s and T_p in Areas 1 and 3, respectively, showing a minimum value at the beginning of the second half of the twenty-first century. This simple form of nonlinear trend detected can be partly attributed to the significant increase in extreme Etesians in 2001–2050 (Anagnostopoulou et al. 2014), causing a consequent increase in extreme wave heights in this period (Galiatsatou and Prinos 2014; Makris et al. 2016; Galiatsatou et al. 2016). However, in the semi-confined Aegean Sea basin, characterised by short fetches, the wave period is more bounded compared to the wave height, thus reacting more slowly to extreme wind forcing and leading to a subsequent decrease in the dependence structure of extreme offshore H_s and T_p until 2050. Dependence of the two offshore variables in Areas 1 and 3 progressively increases in the second half of the twenty-first century, during which extreme Etesian winds enfeeble (especially towards 2100). The dependence parameter of extreme H_s and T_p in Area 2 presents higher-order variability (sixth-order polynomial with

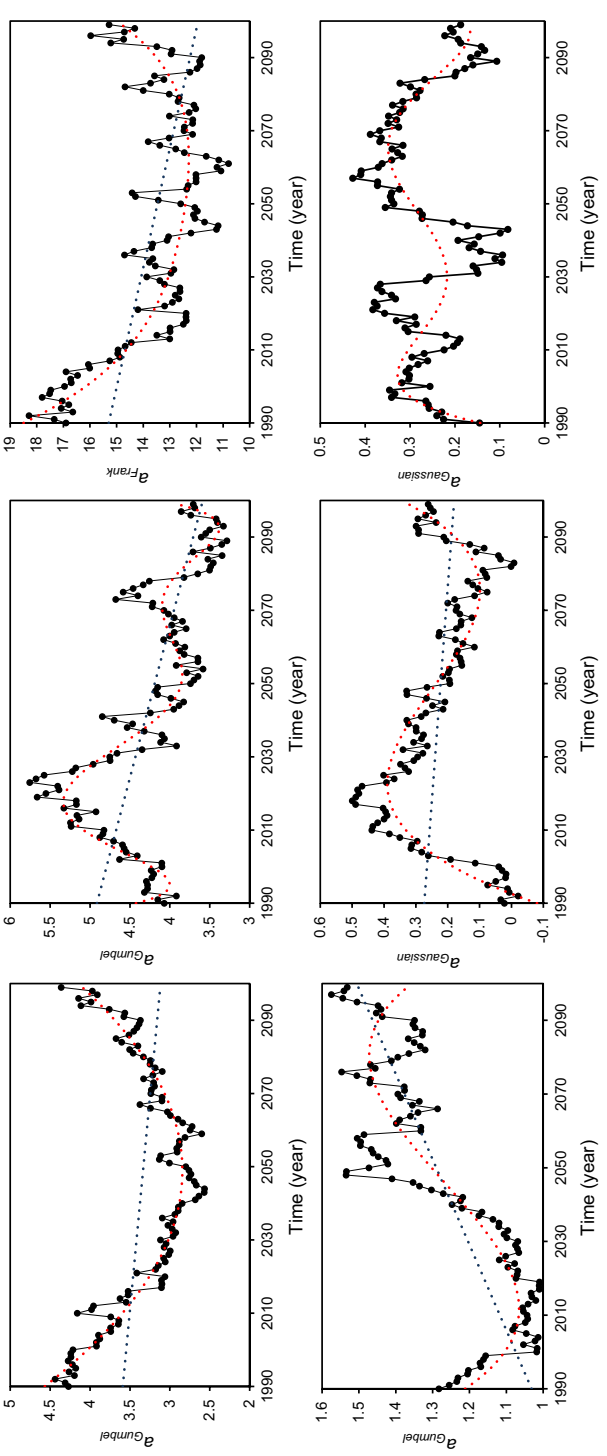

Fig. 5 Dependence parameter of the selected bivariate copulas for H_s and T_p (top row) and η_w and SLH (bottom row) for Areas 1 (first column), 2 (second column) and 3 (third column). Black dotted lines correspond to estimates of the dependence parameter from the 40-year moving windows, while dashed blue and red lines represent statistically significant linear and polynomial trends, respectively

prominent peak around 2020 and secondary lower peak around 2070), possibly due to the oblique (southwestern) orientation of the study area compared to the other two, and thus affected by different winds. The dependence structure of the nearshore variables, η_w and SLH in all study areas, is weaker compared to the respective estimates for the pair of offshore wave parameters. This is mainly attributed to the increased contribution of SLP in generating extreme SLH in the Aegean Sea, which varies with location and time period considered (Androulidakis et al. 2015). In Areas 1 and 2, the dependence parameter of η_w and SLH is best-fitted by a third-order polynomial trend, showing quite an opposite variation in the two areas. Finally, a fifth-order polynomial trend has been selected to model the dependence parameter of the Gaussian copula in Area 3, characterised by a bimodal variation peaking around 2000 and 2070, periods when northerly winds probably invigorate, based on the Two-Step Cluster Analysis (TSCA) of Anagnostopoulou et al. (2014).

Considering events with a low probability of exceedance, the temporal variation in the joint exceedance probability of H_s and T_p, and η_w and SLH can be extracted by constructing joint exceedance probability isolines, considering the temporal variations detected in the marginal distributions of the studied variables as well as in their dependence structure. In the present work, the polynomial functions selected for the marginal distributions of offshore and nearshore variables, and for the dependence structure of the data were used to assess the joint estimates of the studied marine variables corresponding to a joint return period of 100 years (joint exceedance probability $P_E = 0.01$). Figures 6, 7 and 8 present time-dependent joint exceedance probability isolines for each year in the interval 1990–2100 for Areas 1, 2 and 3, respectively.

For Area 1 in the North Aegean Sea, distinct time periods of variability have been detected for both offshore and nearshore bivariate data. During 1990–2060, H_s marginal return level estimates increased up to almost 25%, while the respective T_p marginal values slightly decreased. The tail dependence of the offshore variables also decreased during this interval. During the period 2061–2100, H_s and T_p marginal values decreased from past values up to 23% and 10%, respectively, while upper tail dependence of the two variables increased with time until the end of the twenty-first century. The bivariate nearshore data of η_w and SLH presented four main periods of variability. In the first 10 years, SLH marginal return level estimates gradually decreased up to 16%, while η_w presented an increase

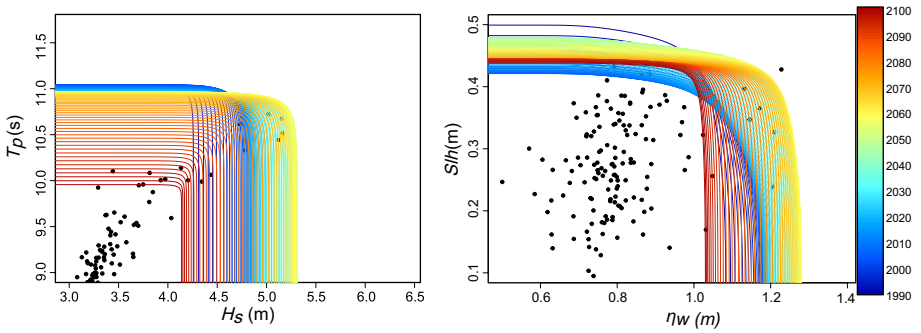

Fig. 6 Time-dependent joint exceedance probability isolines for an exceedance probability $P_E = 0.01$ for the bivariate data of H_s and T_p (left panel) and η_w and SLH (right panel) at Area 1 in the North Aegean Sea. The colour bar refers to the last year of each 40-year window related to the period 1990–2100. The left and right panels correspond to the offshore pair of H_s and T_p, and the nearshore pair of η_w and SLH, respectively. The points correspond to the bivariate observations of the entire sample

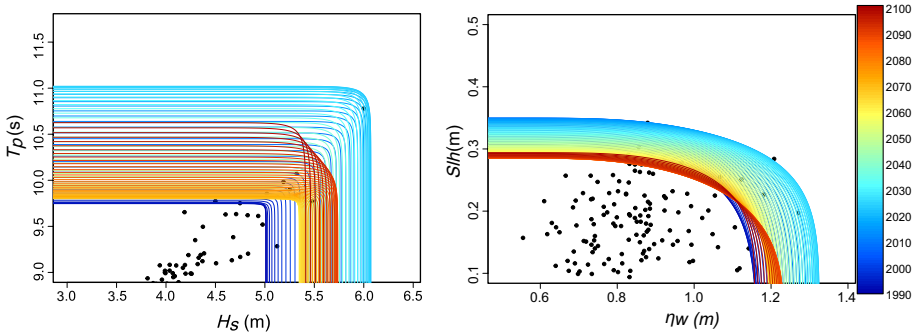

Fig. 7 Time-dependent joint exceedance probability isolines for an exceedance probability $P_E = 0.01$ for the bivariate data of H_s and T_p (left panel) and η_w and SLH (right panel) at Area 2 in the Central Aegean Sea. The colour bar refers to the last year of each 40-year window related to the period 1990–2100. The left and right panels correspond to the offshore pair of H_s and T_p, and the nearshore pair of η_w and SLH, respectively. The points correspond to the bivariate observations of the entire sample

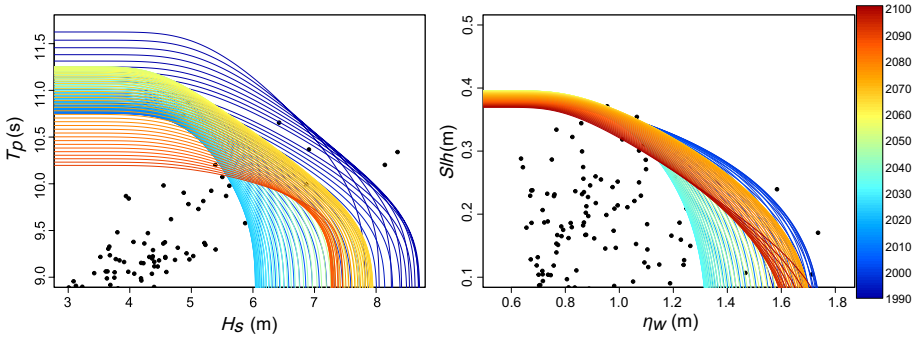

Fig. 8 Time-dependent joint exceedance probability isolines for an exceedance probability $P_E = 0.01$ for the bivariate data of H_s and T_p (left panel) and η_w and SLH (right panel) at Area 3 in the South Aegean Sea. The colour bar refers to the last year of each 40-year window related to the period 1990–2100. The left and right panels correspond to the offshore pair of H_s and T_p, and the nearshore pair of η_w and SLH, respectively. The points correspond to the bivariate observations of the entire sample

of almost 9%. During 2001–2040, both η_w and SLH marginal return level estimates and the dependence structure of the two variables progressively increased compared to past values (stronger upper tail dependence), revealing quite an increasing contribution of the wind field in generating extreme storm surges over time. In the next 20 years (2041–2060), marginal estimates of SLH presented a slight decrease compared to magnitudes until 2040, while the respective estimates of η_w and the tail dependence of the nearshore data continued to rise. Finally, in the last four decades of the twenty-first century, marginal estimates of η_w and SLH as well as their tail dependence structure presented a decreasing trend over time.

For Area 2 in the Central Aegean Sea, the bivariate analysis revealed significant temporal variability in the marginal estimates and in the dependence structure of the offshore and nearshore variables. During 1990–2020, H_s and T_p marginal return level estimates increased up to 22% and 13%, respectively, while the dependence structure of the two variables presented a significant increase (stronger upper tail dependence) obtaining

its maximum values at the end of this period. During the period 2021–2060, H_s and T_p marginal values decreased more than 10% from values of the previous period, followed by a quite sharp increase in both offshore variables in the last 40 years of the twenty-first century (apart from a light decrease in H_s in the last 10 years). The bivariate nearshore data of η_w and SLH presented quite similar periods of variability as the offshore variables. During 1990–2020, both η_w and SLH marginal estimates and the dependence structure of the two variables progressively increased, revealing quite an increasing contribution of the wind field in generating extreme storm surges in this period. In the period 2021–2060, marginal estimates of SLH and η_w decreased up to 20% and 11%, respectively, from the peak values of the 1990–2020 period, while the dependence structure of the two variables became weaker. In the last 40 years of the twenty-first century, marginal estimates of both nearshore variables presented very light changes.

For Area 3 in the South Aegean Sea, the interval 1990–2100 can be separated in three periods of variability for both the offshore and nearshore bivariate data. During the first 40 years of this interval (1990–2030), H_s marginal return level estimates decrease more than 30%, while a slight decrease has also been observed in T_p marginal estimates. The dependence parameter of the offshore variables also decreased during this interval. During the subsequent 40 years (2031–2070), H_s marginal return level estimates increased more than 32% compared to past values, and T_p slightly increased ($<5\%$), while the dependence structure of the two variables has been estimated weaker compared to the other studied periods. During the last 30 years (2071–2100), both H_s and T_p marginal estimates decreased up to almost 10% from their initial magnitudes, while the dependence structure of the variables has shown an increasing trend. The nearshore variables analysed in this area revealed quite similar periods of variability to those detected for the offshore variables. In the period 1990–2030, the marginal estimates of η_w decreased up to 25%, while light decreases have been detected for the SLH. During the next 40 years (2031–2070), η_w marginal estimates increased up to 30% from their initial values, SLH marginal values presented quite a weak increasing trend, while the dependence structure of the two variables became stronger, possibly attributed to the increasing contribution of the wind field in generating SLH events. During the last 30 years of the century, dependence of the two nearshore variables η_w and SLH marginal estimates progressively decreased compared to the past (with the exception of the last 10 years where an increasing trend appeared in η_w marginal estimates).

4.3 Estimation of design events for flood sources and extreme total water level

The most likely design events, corresponding to extremes with highest likelihood to occur, were then defined for each joint exceedance probability isoline for both offshore and nearshore pairs of variables. Figure 9 presents the time-dependent most likely design estimates of offshore H_s and T_p and nearshore SLH for all areas. It includes most likely events extracted using nonlinear parametric trends in the marginals and in the dependence parameter of the bivariate data, as well as events extracted by mere application of moving windows for the estimation of marginals and dependence functions of the available data. Results in Fig. 9 emphasise the necessity of using nonlinear trends in the analysis to reproduce the variability of extreme offshore and nearshore marine conditions within the study period. Considering instead linear trends in the marginals and the dependence function of marine variables would result in losing important information on temporal variability of extremes, location of highest peaks in time, as well as

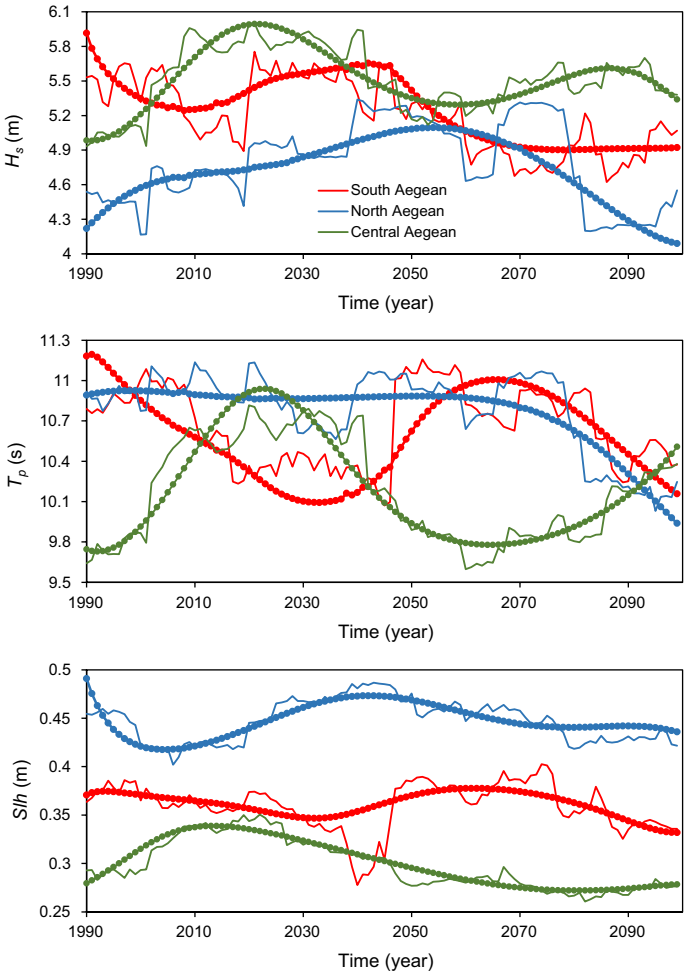

Fig. 9 Time-dependent estimates of the most likely event of offshore H_s (top panel) and T_p (middle panel) and nearshore SLH (*lower panel*) *at Areas 1* (*blue plots*) *in the North* Aegean Sea, 2 (green plots) in the central Aegean Sea and 3 (red plots) in the South Aegean Sea. Solid lines represent the most likely events extracted without any parametric trends in the marginals and in the dependence parameter of the bivariate data, while the lines with marks consider all fitted parametric trends

on underestimation of important most likely design events. It should be noted that most likely design events of η_w are not presented in Fig. 9 to avoid confusion of the reader, since the variable has been only partially included as a separate component in assessing TWL (see below the inclusion of the surf beat component in TWL). In the following, the variability of most likely design events is based on the *Percentage Difference* of their distributions; thus, the term "variations" refers to a ratio of max–min subtraction to the average of marginal values of extremes.

For Area 1 (North Aegean), the most likely design events of H_s, T_p and SLH presented 25%, 10% and almost 20% variations, respectively. The maximum H_s most likely estimate appeared in the second half of the twenty-first century, around 2060, when

including the parametric trends in the marginal parameters and the dependence structure of the offshore variables. Otherwise, the most likely H_s estimates presented a bimodal behaviour with pronounced peaks for a short period before and after the middle of the century. T_p most likely estimates for Area 1 did not present any distinct trend in the first half of the twenty-first century, while they seemed to decrease rapidly form their incipient values and almost linearly during the period 2070–2100. SLH most likely events presented more than 16% variations during the studied time period, when parametric trends were included in the marginal distributions and the dependence structure of the nearshore variables, while the maximum SLH estimates were observed just before the middle of the twenty-first century.

For Area 2 (Central Aegean), offshore H_s most likely estimates presented two distinct peaks, a pronounced one around 2020 and a lower one before the end of the century (around 2085). Variations in H_s estimates approximated 20% (almost 18.5% when including parametric trends in the marginal distributions and the dependence parameter of the offshore variables), while variations in T_p estimates reached 12%. The most likely T_p estimates also peaked around 2020, while they progressively increased in the last 30 years of the century compared to their values of previous periods. SLH variations during the studied time period approximated 30% in the case of ignoring parametric trends for nearshore variables and almost 22% when such trends were included in the analysis.

For Area 3 (South Aegean), the most likely design events of H_s, T_p and SLH presented almost 22%, 10% and 37% variations, respectively. H_s most likely estimates decreased in the second half of the twenty-first century, while T_p estimates increased quite sharply in 2031–2070 compared to previous periods and decreased rapidly during 2071–2100. Therefore, peaks in the most likely estimates of the two offshore variables did not coincide neither did their trending behaviour for almost the entire twenty-first century. The variation in the most likely nearshore SLH estimates during the studied time period appeared quite similar to the one of the offshore T_p, revealing a resembling behaviour of extreme long waves and intense storm surges. When including parametric trends, SLH variations during the studied period reached 14%, showing two distinct peaks at the beginning of the twenty-first century and around 2060.

The TWL at the shoreline, η_t, is estimated via Eq. 2 in the present work as a sum of the wave-induced run-up calculated by means of the most likely H_s and T_p, the most likely SLH in the nearshore area, a certain proportion of the most likely η_w corresponding to the surf beat, η_{sb}, an estimate of MSLR considered equal to almost 2.5 mm/year and an approximation of the highest HAT in three specific areas of the Aegean Sea basin. The surf beat component, η_{sb}, is calculated as a certain proportion of the most likely design η_w event. This proportion varies between 1990 and 2100, based on the estimated contribution of η_{sb} to η_w for each year in the initial dataset used for analysing marginal distribution functions and dependence structure of the nearshore variables (η_{sb} ranging from 14 to 26% of η_w). The wave-induced run-up (including the wave set-up) has been estimated for selected beach profiles at all coastal areas under study, the coastal zone of Alexandroupolis city in Area 1, the coastal zone of Eresos in Area 2 and the coastal zone of the city of Heraklion in Area 3.

Figure 10 presents η_t in the interval 1990–2100 for three selected coastal profiles in Areas 1, 2 and 3. For the selected profile in the coastal area of Alexandroupolis (Area 1), η_t varied more than 17% in the interval 1990–2100 with the highest estimates observed in the second half of the twenty-first century. When parametric trends in the marginal distributions of the marine variables and in their dependence structure were included in the joint probability analysis, the highest η_t estimates appeared around 2060, while when such trends

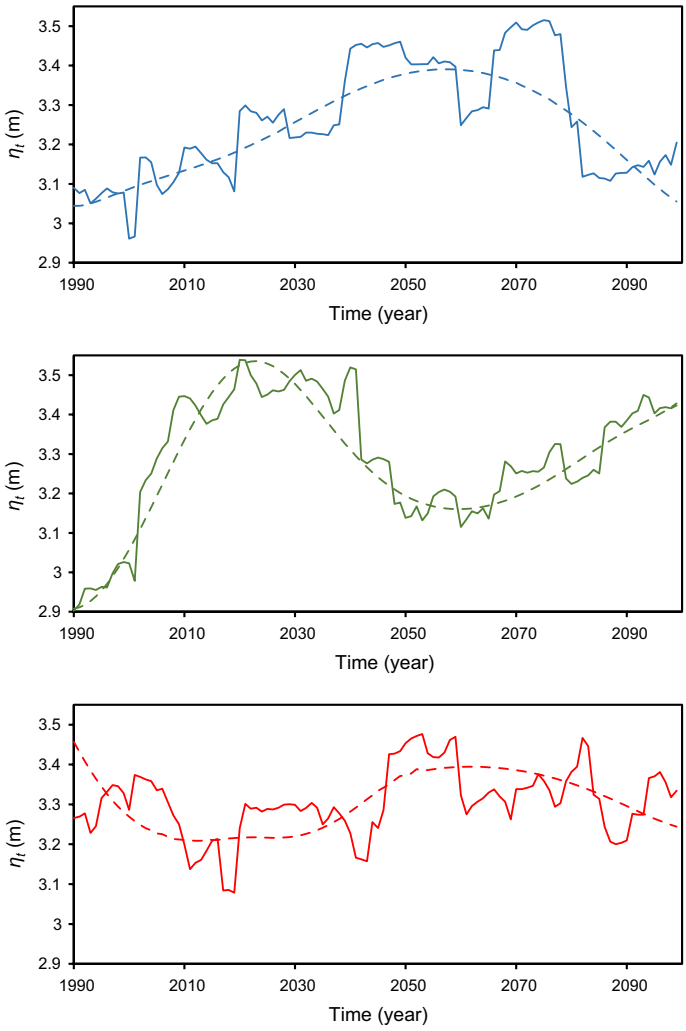

Fig. 10 Time-dependent estimates of the TWL at the shoreline, η_t, at selected profiles in coastal Areas 1 (Alexandroupolis; top panel), 2 (Eresos bay in Lesvos; central panel) and 3 (Heraklion in Crete; bottom panel). Solid lines represent estimates of η_t with time (1990–2100) without any parametric trends in the marginals and in the dependence parameter of the bivariate offshore and nearshore data, while the dashed lines consider all best-fitted parametric trends

were not considered the highest estimates of the hazard appeared in 2070–2075. The water level raised from the beginning of the study period until after the middle of the twenty-first century and then decreased quite rapidly compared to the previous period, approaching the levels of the 1990–2000 period at the end of the twenty-first century. The variations in η_t presented similar trends to those of the offshore most likely design H_s, probably indicating a mostly wave-driven flood risk in the North Aegean coastal zone.

For the selected profile in the coastal area of Eresos in Lesvos (Area 2), η_t variations exceeded 20% in 1990–2100. Maximum values of the TWL at the shoreline appeared just

after 2020 (when parametric trends were not included in the marginals and the dependence structure of the marine variables two other peaks in η_t appeared in 2030 and 2040). The η_t profile showed quite a steep increase in the period 1990–2020, followed by a decrease until the mid-twenty-first century and a subsequent increase until the end of it. Variations in η_t presented a similar trending behaviour to all H_s, T_p and SLH in the area; however, the wave parameters, and especially T_p, seemed to have a stronger influence on them. Even if peak η_t estimates were quite close, variations in η_t in Area 2 seemed to differ significantly from those in Area 1. The most pronounced changes focused on the time of appearance of the maximum η_t (first and second half of the twenty-first century in Area 2 and Area 1, respectively), as well as trends appearing during the last 30 years of the twenty-first century (decreasing and increasing in Area 1 and Area 2, respectively). Therefore, the coastal flood risk in the Central Aegean seems probably dependent in an intermixed way on all sea state and storm-driven parameters, i.e. susceptible to both waves and surges.

Finally, for the selected profile in the coastal area of Heraklion in Crete (Area 3) η_t varied more than 12% in the period 1990–2100. The highest values of η_t appeared around 2060 when parametric trends were included in the marginal distributions and the dependence parameters of the marine variables. When such trends were not included in the joint probability analysis, the highest η_t estimates appeared in the period 2050–2060 and just after 2080. The values of η_t increased after 2030 and were kept quite high in the second half of the twenty-first century. Variations in T_p and in SLH seemed to have a pronounced influence on η_t, while H_s seemed less correlated with η_t, especially compared to the other two study areas of the Aegean Sea. Hence, by combining the latter with the northerly orientation of the coastal zone in Area 3, possible flood hazards in the future are estimated to be caused by approximately meridional storm tracks inducing high surges and energetic sea states of rather extreme low-frequency spectral wave bands. The highest estimates of η_t did not differ significantly from those in the other two areas; however, trends detected in its variability were unique. It should be noted that variations in η_t in this area were not as pronounced as in the other two areas.

5 Conclusions

In the present study, a recent novel approach has been further developed and applied to selected Greek coastal areas of the Aegean Sea in order to investigate the changes in the joint probabilities of extreme marine variables with time and to assess design TWL at the shoreline under the effect of a possible realisation of climate change. The dependence structure of the studied offshore and nearshore variables has been modelled using copulas. The nonstationary GEV distribution has been utilised to model the marginal distribution functions of all variables, fitted to 40-year moving windows. All parameters of the GEV were tested for statistically significant trends. Different copula functions were fitted to model the dependence structure of the data. The nonstationarity of the dependence structure of the studied variables was also investigated. Design events of offshore wave parameters and nearshore storm surges and wave-induced sea levels on the shoreline were extracted, and finally, TWL estimates at the shoreline were produced for selected beach profiles in three characteristic study areas of the Aegean Sea.

The multivariate sea state conditions used in the present nonstationary copula-based approach were selected based on the principal sources of coastal flooding and not on the associated response function (the TWL), recognising the domination of wave

contribution on the flooding hazard in the coastal areas of the Aegean Sea. Therefore, defining our multivariate sea storm events based on maximum wave events, considering strict directional and durational constraints, we achieved to include the highest possible simultaneous realisations of the individual variables contributing to TWL and the flooding hazard. This was verified by the results of the present analysis, where wave-induced water levels account for more than 70%, 76% and 74% of the extreme TWL signal in Areas 1 (North Aegean Sea), 2 (Central Aegean Sea) and 3 (South Aegean Sea), respectively. However, it should be noted that in environments where the tide, the storm surge, and large wave events significantly enhance the elevation of TWL at the shoreline, a more reliable procedure to select compound events is oriented to maximising the response function used for coastal flooding, defined as the extreme TWL at the shoreline. This definition seems to be in better agreement with the IPCC SREX report (Seneviratne et al. 2012), where a compound event is an extreme impact that depends on multiple statistically dependent variables or events (Leonard et al. 2014).

The processes that cause extreme waves and storm surges are nonstationary. In the present work, nonstationarity on time scales longer than the seasonal or interannual is examined, possibly attributed to climate change. The nonstationary analysis of the marginal distributions of all marine variables revealed statistically significant trends in all parameters of the GEV at the selected areas of the Aegean Sea. Negative or positive linear trends were detected in almost all parameters, while the best-fitted polynomial trends were of third to fifth order. Similar polynomial trends resulted for the offshore H_s and associated nearshore η_w in all three studied areas of the Aegean Sea. Statistically significant polynomial trends were also detected in the dependence structure of both offshore and nearshore bivariate data. Second-order polynomial trends were selected to fit the dependence structure of H_s and T_p in the studied areas of the North and South Aegean Seas (Areas 1 and 3), while the dependence structure of the offshore variables in the Central Aegean Sea (Area 2) presented a higher-order polynomial trend. The dependence structure of nearshore η_w and SLH was best-fitted by third- or fifth-order polynomials. The aforementioned trends in the North Aegean coastal zone can be probably attributed to the decreased relative contribution of severe zonal wind components to the generation of extreme wave heights in the second half of the twenty-first century (Galiatsatou et al. 2016). Lower means and variance of extremes, but stronger tails in the Central Aegean during the middle of the twenty-first century might be possibly attributed to the rise of Etesians (i.e. local strong meridional winds; Maheras 1980) and their tendency to deviate off their main course in the central parts of the Aegean. In the South Aegean, Cretan coastal zones, the influence of a dense island cluster (i.e. the Cyclades) was considered responsible for any effects on trends of the GEV parameters, mainly due to diffraction of spectral waves of lower-frequency bands having prominent impacts on wave height extremes (Galiatsatou et al. 2016). Differences in variability of extreme wave periods and heights can be possibly attributed to the combination of multiple changes in wind patterns throughout the twenty-first century (Anagnostopoulou et al. 2014) and the fetch-limited character of wind wave generation in most parts of the Aegean.

For the studied area in the North Aegean Sea (Area 1), the joint exceedance probability analysis of offshore wave parameters revealed two main periods of variability, 1990–2060 and 2061–2100. The bivariate nearshore data of η_w and SLH presented four main periods of variability, while a possible increase in the contribution of the wind field in generating extreme storm surges over time has been detected in 2001–2060, due to the progressive increase in the dependence structure of the two variables (stronger upper tail dependence).

The highest TWL at the shoreline has been estimated in the second half of the twenty-first century, presenting a rapid decrease in the last 30 years of it. Variations in η_t in this area exceeded 17% during the studied period and presented similar trends to variations in offshore H_s.

In the Central Aegean Sea (Area 2), significant temporal variability in the marginal estimates and in the dependence structure of the offshore and nearshore variables has been detected. Three main periods of variability in the marginal distributions and the dependence structure of both the offshore and nearshore marine variables have been detected (1990–2020, 2021–2060 and 2061–2100). A possible increase in the contribution of the wind field in generating high storm surges has been detected in the first 30 years of the study period. The highest TWL at the shoreline has been estimated in the first half of the twenty-first century (around 2020), followed by a decrease until the mid-twenty-first century and a subsequent increase until the end of it. Variations in η_t presented a similar trending behaviour to all H_s, T_p and SLH in the area; however, the wave parameters, and especially T_p, seemed as expected to be highly correlated with the final estimates of the TWL and the conclusive flooding hazard, since the run-up (major contributor to TWL) parameterisation of Stockdon et al. (2006) is highly dependent on wave periods in comparison with wave heights.

For the studied area in the South Aegean Sea (Area 3), three main periods of variability in the marginal distributions and the dependence structure of the offshore and nearshore marine variables were detected (1990–2030, 2031–2070 and 2071–2100). During the period 2031–2070, the dependence structure of the nearshore (η_w and SLH) variables became stronger, possibly resulting from the increased contribution of the wind field in generating high storm surges. The TWL at the shoreline was estimated to increase after 2030 and was assessed quite high in the second half of the twenty-first century. The highest values of η_t were calculated around the middle of the century, while estimated trends, especially in $T_{p,}$ seemed to have a significant influence on extreme η_t estimates. In opposition to the high correlations of η_t and H_s assessed in the North Aegean Sea, in the studied area of the South Aegean Sea wave lengths and SLH were highly correlated with TWL at the shoreline.

The spatial differentiations of the patterns of extreme marine variables reveal the following conclusions, based on the intense topographical variety of the Aegean archipelago. In the North Aegean (with sparse large islands), the peaks of extreme wave characteristics are estimated to occur around 2060 while storm surges tend to be intensified during 2040–2050. These findings hinge on a more sophisticated (detailed and physically based) approach compared to former studies in the area (Galiatsatou and Prinos 2014, 2015; Makris et al. 2016), which assessed climate change effects on extreme wave heights and storm surges (univariate EVA for monthly maxima of H_s and SLH) in the area, considering nonstationarity only on the seasonal scale of the different processes (each GEV parameter represented as harmonic function of time; Menéndez et al. 2009) for three a priori defined 50-year periods (1951–2000, 2001–2050, 2051–2100). These new results imply the rise of extreme southerly winds in the Aegean Sea towards the middle of the twenty-first century and beyond (Vagenas et al. 2017). In the South Aegean, the Aeolian patterns show a mild rise of northerly extreme winds after the first half of the twenty-first century, which might lead to an increase in extreme peak periods and respective storm surges that are slightly intensified. Nevertheless, due to the complex dense insular formation of the Cyclades, the random wave fields are prone to diffraction, and this seems to cause a slight drop in the significant wave height extremes. These findings are in line with a projected significant increase in extreme Etesians in 2001–2050, probably causing a consequent increase in

extreme wave heights in this period. The coastal zones in the south and north Aegean Sea (Areas 1 and 3) are mostly influenced by the latter. Rather clear patterns of storminess attenuation in the second half of the twenty-first century are found and thus corroborate the climate change signals of earlier studies (Galiatsatou and Prinos 2014, 2015; Makris et al. 2016). Further analysis on dependencies of extreme marine variables on synoptic scale wind and SLP patterns (driving mechanisms of coastal flood sources) could be achieved only through a more sophisticated approach, such as PCA, Empirical Orthogonal Functions (EOFs) or Self-Organising Maps (SOMs) for weather patterns, which is out of the scope of the present paper. The proposed approach of EV calculation, including nonstationarity in marginal distributions and dependence structure, bivariate analysis of extremes and associated parameters, and incorporation of coastal sea states, establishes estimations of return levels for nearshore marine variables.

As coastal flooding or coastal defence failure are hazards produced by a combination of wave parameters and components of the nearshore sea level, an understanding of the dependencies between the variables could permit to more accurately predict their joint probability of occurrence and to assess any related risks more efficiently and with greater confidence. Since the studied offshore and nearshore marine variables are neither independent nor fully dependent, a joint probability approach, considering the dependence of the input variables, as well as the distributions and extremes of the individual variables, can significantly contribute to unequivocal estimates of design quantities for coastal defences and of the flooding hazard and associated flood risk. The benefits of a joint probability approach conducted for marine processes of similar nature, magnitude and spatial scales both in offshore and in nearshore areas of selected coastal locations, combined with the developed nonstationary copula-based framework to assess the possible impacts of climate change on a coastal process, allow for an alternative estimation of extreme sources of flooding and their statistical dependencies. Thus, a more comprehensive representation of variability and long-term trends in the TWL process is feasible for a given atmospheric forcing which represents a possible realisation of the future climate.

The work presented in the paper summarises a first approach to the nonstationary modelling of offshore and nearshore marine variables to assess design water levels at the shoreline in a changing climate. The methodology presented could be further evolved by selecting design events using more advanced approaches, more physically based and better oriented to flooding hazards. Also, the accuracy of the cumulative results of the study could be enhanced by incorporating ensembles of marine data, produced under several different climate change scenarios, in the EVA.

Acknowledgements This research has been co-financed by the European Union (European Social Fund—ESF) and Greek national funds through the Operational Program "Education and Lifelong Learning" of the National Strategic Reference Framework (NSRF)—Research Funding Program: Thales. Investing in knowledge society through the European Social Fund (Project CCSEAWAVS: Estimating the effects of climate change on sea level and wave climate of the Greek seas, coastal vulnerability and safety of coastal and marine structures). The second and fourth authors are IKY-SIEMENS post-doc and Ph.D. research fellows under the programme "IKY-SIEMENS excellence scholarships for postdoctoral and doctoral research in Greece by the State Scholarships Foundation (SSF/IKY) (Grant No. 24528/SR) academic year 2016–2017".

References

Adloff F, Somot S, Sevault F, Jordà G, Aznar R, Déqué M, Herrmann M, Marcos M, Dubois C, Padorno E, Alvarez-Fanjul E, Gornis D (2015) Mediterranean Sea response to climate change in an ensemble of twenty first century scenarios. Clim Dyn 45(9–10):2775–2802

AghaKouchak A, Bárdossy A, Habib E (2010) Conditional simulation of remotely sensed rainfall data using a non-Gaussian v-transformed copula. Adv Water Resour 33(6):624–634

Akaike H (1974) A new look at the statistical model identification. IEEE Trans Autom Control 19(6):716–723

Anagnostopoulou C, Zanis P, Katragkou E, Tegoulias I, Tolika K (2014) Recent past and future patterns of the Etesian winds based on regional scale climate model simulations. Clim Dyn 42(7–8):1819–1836

Androulidakis YS, Kombiadou KD, Makris CV, Baltikas VN, Krestenitis YN (2015) Storm surges in the Mediterranean Sea: variability and trends under future climatic conditions. Dyn Atmos Oceans 71:56–82

Baldock TE (2006) Long wave generation by the shoaling and breaking of transient wave groups on a beach. Proc R Soc A 462:1853–1876

Baldock TE, Huntley DA, Bird PAD, O'Hare T, Bullock GN (2000) Breakpoint generated surf beat induced by bichromatic wave groups. Coast Eng 39(2–4):213–242

Bardet L, Duluc CM, Rebour V, L'Her J (2011) Regional frequency analysis of extreme storm surges along the French coast. Nat Hazard Earth Syst Sci 11(6):1627–1639

Bender J, Wahl T, Jensen J (2014) Multivariate design in the presence of non-stationarity. J Hydrol 514:123–130

Benetazzo A, Fedele F, Carniel S, Ricchi A, Bucchignani E, Sclavo M (2012) Wave climate of the Adriatic Sea: a future scenario simulation. Nat Hazard Earth Syst Sci 12(6):2065–2076

Booij N, Ris RC, Holthuijsen LH (1999) A third-generation wave model for coastal regions. 1. Model description and validation. J Geophys Res 104:7649–7666

Bulteau T, Lecacheux S, Lerma AN, Paris F (2013) Spatial extreme value analysis of significant wave heights along the French coast. In: Proceedings of the EVAN2013, Siegen, Germany

Butler A, Heffernan JE, Tawn JA, Flather RA (2007) Trend estimation in extremes of synthetic North Sea surges. J R Stat Soc Ser C 56(4):395–414

Callaghan DP, Nielsen P, Short A, Ranasinghe R (2008) Statistical simulation of wave climate and extreme beach erosion. Coast Eng 55(5):375–390

Carillo A, Sannino G, Artale V, Ruti PM, Calmanti S, Dell'Aquila A (2012) Steric sea level rise over the Mediterranean Sea: present climate and scenario simulations. Clim Dyn 39(9–10):2167–2184

Casas-Prat M, Sierra JP (2011) Future scenario simulations of wave climate in the NW Mediterranean Sea. J Coastal Res SI 64:200–204

Casas-Prat M, Sierra JP (2013) Projected future wave climate in the NW Mediterranean Sea. J Geophys Res-Oceans 118(7):3548–3568

Chambers JM (1992) Chapter 4 of statistical models in S. In: Chambers JM, Hastie TJ (eds) Linear models. Wadsworth & Brooks/Cole, Belmont

Chebana F, Ouarda TBMJ, Duong TC (2013) Testing for multivariate trends in hydrologic frequency analysis. J Hydrol 486:519–530

Coelho C, Lopes D, Freitas P (2009) Morphodynamics classification of Areão Beach, Portugal. J Coast Res SI 56:34–38

Coles S (2001) An introduction to statistical modelling of extreme values. Springer Series in Statistics. Springer, Berlin

Coles S, Tawn J (2005) Bayesian modelling extreme surges on the UK east coast. Philos Trans A Math Phys Eng Sci 363:1387–1406

Conte D, Lionello P (2013) Characteristics of large positive and negative surges in the Mediterranean Sea and their attenuation in future climate scenarios. Glob Planet Change 111:159–173

Corbella A, Stretch DD (2013) Simulating a multivariate sea storm using Archimedean copulas. Coast Eng 76:68–78

De Haan L, De Ronde J (1998) Sea and wind: multivariate extremes at work. Extremes 1:7–45

De Kort J (2007) Modelling tail dependence using copulas-literature review. http://ta.twi.tudelft.nl/nw/users/vuik/numanal/kort_scriptie.pdf. Accessed 23 Dec 2017

De Michele C, Salvadori G, Passoni G, Vezzoli R (2007) A multivariate model of sea storms using copulas. Coast Eng 54(10):734–751

Dean R, Dalrymple RA (2002) Coastal processes with engineering applications. Cambridge University Press, New York

Dickinson R, Errico R, Giorgi F, Bates G (1989) A regional climate model for the western United States. Clim Change 15(3):383–422
Ferreira JA, Guedes Soares C (2002) Modelling bivariate distributions of significant wave height and mean period. Appl Ocean Res 24:31–45
Gaertner MA, Jacob D, Gil V, Dominguez M, Padorno E, Sanchez E, Castro M (2007) Tropical cyclones over the Mediterranean Sea in climate change simulations. Geophys Res Lett 34(14):L14711
Galiatsatou P (2007) Joint exceedance probabilities of extreme waves and storm surges. In: XXXIII IAHR Congress, pp 780 (abstract), JFK Competition
Galiatsatou P, Prinos P (2008) Non-stationary point process models for extreme storm surges. In: Flood risk management: research and practice: proceedings of the Floodrisk 2008. Oxford, pp 1045–1054
Galiatsatou P, Prinos P (2014) Analysing the effects of climate change on wave height extremes in the Greek Seas. In: Lehfeldt R, Kopmann R (eds) Proceedings of the ICHE 2014, Hamburg© 2014 Bundesanstalt für Wasserbau, pp 773–781. ISBN 978-3-939230-32-8
Galiatsatou P, Prinos P (2015) Estimating the effects of climate change on storm surge extremes in the Greek Seas. In: Proceedings of the 36th IAHR World Congress, The Hague
Galiatsatou P, Prinos P (2016) Joint probability analysis of extreme wave heights and storm surges in the Aegean Sea in a changing climate. In: E3S Web of Conferences, vol 7. EDP Sciences, p 02002. https://doi.org/10.1051/e3sconf/20160702002
Galiatsatou P, Anagnostopoulou C, Prinos P (2016) Modelling nonstationary extreme wave heights in present and future climates of Greek Seas. Water Sci Eng 9(1):21–32
Gaslikova L, Grabemann I, Groll N (2013) Changes in North Sea storm surge conditions for four transient future climate realizations. Nat Hazards 66(3):1501–1518
Genest C, Rémillard B, Beaudoin D (2009) Goodness-of-fit tests for copulas: a review and a power study. Insur Math Econ 44(2):199–213
Goda Y (2000) Random sea and design of maritime structures, 2nd edn. World Scientific, Singapore
Gouldby B, Méndez FJ, Guanche Y, Rueda A, Mínguez R (2014) A methodology for deriving extreme nearshore conditions for structural design and flood risk analysis. Coast Eng 88:15–24
Gräler B, van den Berg MJ, Vandenberghe S, Petroselli A, Grimaldi S, De Baets B, Verhoest NEC (2013) Multivariate return periods in hydrology: a critical and practical review focusing on synthetic design hydrograph estimation. Hydrol Earth Syst Sci 17:1281–1296
Grimaldi S, Serinaldi F (2006) Design hyetographs analysis with 3-copula function. Hydrol Sci J 51(2):223–238
Heffernan JE, Tawn JA (2004) A conditional approach for multivariate extreme values. J R Stat Soc Ser B 66(3):497–546 **(with discussion)**
Hipel KW, McLeod AI (2005) Time Series Modelling of Water Resources and Environmental Systems. Electronic reprint of the book originally published in 1994, http://www.stats.uwo.ca/faculty/aim/1994Book/. Accessed 23 Dec 2017
Hosking JRM (1990) L-moments: analysis and estimation of distributions using linear combinations of order statistics. J R Stat Soc Ser B 52:105–124
Hosking JRM, Wallis JR (1997) Regional frequency analysis: an approach based on L-moments. Cambridge University Press, Cambridge
Hsu CH, Olivera F, Irish JL (2018) A hurricane surge risk assessment framework using the joint probability method and surge response functions. Nat Hazards 91(1):7–28
IPCC (2007) Climate change 2007: the scientific basis. In: Solomon S et al (eds) Contribution of Working Group I to the Fourth Assessment Report of the Intergovernmental Panel on Climate change. Cambridge University Press, New York
IPCC (2012) Managing the risks of extreme events and disasters to advance climate change adaptation. In: Field CB et al (eds) A Special Report of Working Groups I and II of the Inter-governmental Panel on Climate change. Cambridge University Press, Cambridge
IPCC (2013) Climate change 2013: the physical science basis. In: Stocker TF, Qin D, Plattner G-K, Tignor M, Allen SK, Boschung J, Nauels A, Xia Y, Bex V, Midgley PM (eds) Contribution of Working Group I to the Fifth Assessment Report of the Intergovernmental Panel on Climate Change. Cambridge University Press, Cambridge, p 1535
Janga Reddy M, Ganguli P (2012) Application of copulas for derivation of drought severity–duration–frequency curves. Hydrol Process 26(11):1672–1685
Jiang C, Xiong L, Xu CY, Guo S (2015) Bivariate frequency analysis of nonstationary low-flow series based on the time-varying copula. Hydrol Process 29(6):1521–1534
Joe H, Xu JJ (1996) The estimation method of inference functions for margins for multivariate models. Working paper, Department of Statistics, University of British Columbia

Jonathan P, Randell D, Wu Y, Ewans K (2014a) Return level estimation from non-stationary spatial data exhibiting multidimensional covariate effects. Ocean Eng 88:520–532
Jonathan P, Ewans K, Randell D (2014b) Non-stationary conditional extremes of northern North Sea storm characteristics. Environmetrics 25(3):172–188
Kao SC, Govindaraju RS (2008) Trivariate statistical analysis of extreme rainfall events via the Plackett family of copulas. Water Resour Res 44(2):W02415. https://doi.org/10.1029/2007WR006261
Kapelonis ZG, Gavriliadis PN, Athanassoulis GA (2015) Extreme value analysis of dynamical wave climate projections in the Mediterranean Sea. Proc Comput Sci 66:210–219
Krestenitis YN, Androulidakis YS, Kontos YN, Georgakopoulos G (2011) Coastal inundation in the north-eastern Mediterranean coastal zone due to storm surge events. J Coast Conserv 15(3):353–368
Krestenitis Y, Androulidakis Y, Kombiadou K, Makris C, Baltikas V (2014) Modeling storm surges in the Mediterranean Sea under the A1B climate scenario, Proc. 12th International Conference on Meteorology, Climatology and Atmospheric Physics (COMECAP), Heraklion (Crete), Greece, 28–31 May 2014, pp 91–95
Kwon HH, Lall U (2016) A copula-based nonstationary frequency analysis for the 2012–2015 drought in California. Water Resour Res 52(7):5662–5675
Leonard M, Westra S, Phatak A, Lambert M, van den Hurk B, McInnes K, Risbey J, Schuster S, Jakob D, Stafford-Smith M (2014) A compound event framework for understanding extreme impacts. WIRES Clim Change 5:113–128
Li F, Van Gelder PHAJM, Ranasinghe R, Callaghan DP, Jongejan RB (2014) Probabilistic modelling of extreme storms along the Dutch coast. Coast Eng 86:1–13
Lionello P, Cogo S, Galati MB, Sanna A (2008) The Mediterranean surface wave climate inferred from future scenario simulations. Glob Planet Change 63:152–162
Lopeman M, Deodatis G, Franco G (2015) Extreme storm surge hazard estimation in lower Manhattan. Nat Hazards 78(1):355–391
Maheras P (1980) The problem of Etesians [Le probleme des Etesiens]. Mediterranée 40:57–66
Makris CV, Krestenitis YN (2009) Free educational software on maritime hydrodynamics, coastal engineering and oceanography. In: Proceedings of the 9th Pan-Hellenic symposium of oceanography and fisheries, vol 1, pp 546–551 **(in Greek)**
Makris CV, Androulidakis YS, Krestenitis YN, Kombiadou KD, Baltikas VN (2015) Numerical modelling of storm surges in the Mediterranean Sea under climate change. In: Proceedings of the 36th IAHR World Congress, The Hague
Makris C, Galiatsatou P, Tolika K, Anagnostopoulou C, Kombiadou K, Prinos P, Velikou K, Kapelonis Z, Tragou E, Androulidakis Y, Athanassoulis G, Vagenas C, Tegoulias I, Baltikas V, Krestenitis Y, Gerostathis T, Belibassakis K, Rusu E (2016) Climate change effects on the marine characteristics of the Aegean and Ionian Seas. Ocean Dyn 66(12):1603–1635
Marcos M, Tsimplis MN (2008) Coastal sea level trends in Southern Europe. Geophys J Int 175(1):70–82
Martucci G, Carniel S, Chiggiato J, Sclavo M, Lionello P, Galati MB (2010) Statistical trend analysis and extreme distribution of significant wave height from 1958 to 1999—an application to the Italian Seas. Ocean Sci 6(2):525–538
Masina M, Lamberti A, Archetti R (2015) Coastal flooding: a copula based approach for estimating the joint probability of water levels and waves. Coast Eng 97:37–52
Mazas F, Hamm L (2017) An event-based approach for extreme joint probabilities of waves and sea levels. Coast Eng 122:44–59
McInnes KL, Macadam I, Hubbert GD, O'Grady JG (2009) A modelling approach for estimating the frequency of sea level extremes and the impact of climate change in southeast Australia. Nat Hazards 51(1):115–137
Méndez FJ, Menéndez M, Luceño A, Losada IJ (2006) Estimation of the long-term variability of extreme significant wave height using a time-dependent Peak Over Threshold (POT) model. J Geophys Res 111(7):C07024
Méndez FJ, Menéndez M, Luceño A, Medina R, Graham NE (2008) Seasonality and duration in extreme value distributions of significant wave height. Ocean Eng 35(1):131–138
Menéndez M, Méndez FJ, Izaguirre C, Luceño A, Losada IJ (2009) The influence of seasonality on estimating return values of significant wave height. Coast Eng 56(3):211–219
Morton ID, Bowers J (1996) Extreme value analysis in a multivariate offshore environment. Appl Ocean Res 8:303–317
Nelsen RB (2006) An introduction to copulas, 2nd edn, Lecture Notes in Statistics. Springer, New York
Plant NG, Stockdon HF (2015) How well can wave runup be predicted? Comment on Laudier et al.(2011) and Stockdon et al.(2006). Coast Eng 102:44–48
Pugh DT (1996) Tides, surges and mean sea-level (reprinted with corrections). John Wiley and Sons

Rai RK, Upadhyay A, Ojha CSP, Lye LM (2013) Statistical analysis of hydro-climatic variables. In: Surampalli RY, Zhang TC, Ojha CSP, Gurjar BR, Tyagi RD, Kao CM (eds) Climate change modelling, mitigation, and adaptation. ASCE, Reston. https://doi.org/10.1061/9780784412718

Repko A, Van Gelder PHAJM, Voortman HG, Vrijling JK (2004) Bivariate description of offshore wave conditions with physics-based extreme value statistics. Appl Ocean Res 26:162–170

Ridder N, de Vries H, Drijfhout S, van den Brink H, van Meijgaard E, de Vries H (2018) Extreme storm surge modelling in the North Sea. Ocean Eng 68:255–272

Roeckner E, Brokopf R, Esch M, Giorgetta MA, Hagemann S, Kornblueh L, Manzini E, Schlese U, Schulzweida U (2006) Sensitivity of simulated climate to horizontal and vertical resolution in the ECHAM5 atmosphere model. J Climate 19(16):3771–3791

Rueda A, Camus P, Tomás A, Vitousek S, Méndez FJ (2016) A multivariate extreme wave and storm surge climate emulator based on weather patterns. Ocean Model 104:242–251

Rutkowska A (2015) Properties of the Cox–Stuart test for trend in application to hydrological series: the simulation study. Commun Stat-Simul Comput. 44(3):565–579

Salvadori G, De Michele C (2010) Multivariate multiparameter extreme value models and return periods: a copula approach. Water Resour Res 46(10):W10501. https://doi.org/10.1029/2009WR009040

Salvadori G, De Michele C, Durante F (2011) Multivariate design via copulas. Hydrol Earth Syst Sci Discuss 8(3):5523–5558

Sánchez-Arcilla A, Gomez-Aguar J, Egozcue JJ, Ortego MI, Galiatsatou P, Prinos P (2008) Extremes from scarce data. The role of Bayesian and scaling techniques in reducing uncertainty. J Hydraul Res 46(2):224–234

Sartini L, Besio G, Cassola F (2017) Spatio-temporal modelling of extreme wave heights in the Mediterranean Sea. Ocean Model 117:52–69

Seneviratne SI, Nicholls N, Easterling D, Goodess CM, Kanae S, Kossin J, Luo Y, Marengo J, McInnes K, Rahimi M, Reichstein M, Sorteberg A, Vera C, Zhang X (2012) Changes in climate extremes and their impacts on the natural physical environment. In: Field CB, Barros V, Stocker TF, Qin D, Dokken DJ, Ebi KL, Mastrandrea MD, Mach KJ, Plattner G-K, Allen SK, Tignor M, Midgley PM (eds) Managing the risks of extreme events and disasters to advance climate change adaptation. A Special Report of Working Groups I and II of the Intergovernmental Panel on Climate Change (IPCC). Cambridge University Press, Cambridge, pp 109–230

Serafin KA, Ruggiero P (2014) Simulating extreme total water levels using a time-dependent extreme value approach. J Geophys Res Oceans 119:6305–6329

Serafin KA, Ruggiero P, Stockdon HF (2017) The relative contribution of waves, tides, and nontidal residuals to extreme total water levels on U.S. West Coast sandy beaches. Geophys Res Lett 44:1839–1847

Shiau JT (2006) Fitting drought duration and severity with two dimensional copulas. Water Resour Manag 20(5):795–815

Short AD (1999) Handbook of beach and shoreface morphodynamics, vol XII. Wiley, New York

Singh VP, Zhang L (2007) IDF curves using the Frank Archimedean copula. J Hydrol Eng 12(6):651–662

Somot S, Sevault F, Déqué M, Crépon M (2008) 21st century climate change scenario for the Mediterranean using a coupled atmosphere–ocean regional climate model. Glob Planet Change 63(2):112–126

Sterl A, Brink HVD, Vries HD, Haarsma R, Meijgaard EV (2009) An ensemble study of extreme storm surge related water levels in the North Sea in a changing climate. Ocean Sci. 5(3):369–378

Stockdon HF, Holman RA, Howd PA, Sallenger AH (2006) Empirical parameterization of setup, swash, and runup. Coast Eng 53:573–588

Tolika K, Anagnostopoulou C, Velikou K, Vagenas C (2016) A comparison of the updated very high resolution model RegCM3_10km with the previous version RegCM3_25km over the complex terrain of Greece: present and future projections. Theor Appl Climatol 126(3–4):715–726

Tsimplis MN (1994) Tidal oscillations in the Aegean and Ionian Seas. Estuar Coast Shelf Sci 39(2):201–208

Tsimplis MN, Proctor R, Flather RA (1995) A two-dimensional tidal model for the Mediterranean Sea. J Geophys Res Oceans 100(C8):16223–16239

Tsimplis MN, Calafat FM, Marcos M, Jordà G, Gomis D, Fenoglio-Marc L, Struglia MV, Josey SA, Chambers DP (2013) The effect of the NAO on sea level and on mass changes in the Mediterranean Sea. J Geophys Res-Oceans 118(2):944–952

Vagenas C, Anagnostopoulou C, Tolika K (2014) Climatic study of the surface wind field and extreme winds over the Greek seas. In: Proceedings of the 12th COMECAP, Heraklion, Greece

Vagenas C, Anagnostopoulou C, Tolika K (2017) Climatic study of the marine surface wind field over the Greek seas with the use of a high resolution RCM focusing on extreme winds. Climate 5(2):29

van Gelder PHAJM, Mai C (2008) Distribution functions of extreme sea waves and river discharges. J Hydraul Res 46(2):280–291

van Gelder PHAJM (1999) Risk-based design of civil structures. Ph.D.-Thesis, University of Technology, Delft

Velikou K, Tolika K, Anagnostopoulou I, Vagenas C (2014) High resolution climate over Greece: assessment and future projections. In: Proceedings of the 12th COMECAP, Heraklion, Greece

Wahl T, Mudersbach C, Jensen J (2012) Assessing the hydrodynamic boundary conditions for risk analyses in coastal areas: a multivariate statistical approach based on copula functions. Nat Hazard Earth Syst Sci 12:495–510

Wahl T, Plant NG, Long JW (2016) Probabilistic assessment of erosion and flooding risk in the northern Gulf of Mexico. J Geophys Res Oceans 121:3029–3043

Yan J (2007) Enjoy the joy of copulas: with a package copula. J Stat Softw 21(4):1–21

Yeh SP, Ou SP, Doong DJ, Kao CC, Hsieh DW (2006) Joint probability analysis of waves and water level during typhoons. In: Proceedings of the 3rd Chinese-German joint symposium on coastal and ocean engineering

Zhong H, van Overloop P-J, van Gelder P (2013) A joint probability approach using a 1-D hydrodynamic model for estimating high water level frequencies in the Dutch Lower Rhine Delta. Nat Hazard Earth Syst Sci 13:1841–1852